

**Interactions between Anterior Thalamus and Hippocampus during  
Different Behavioral States in the Rat**

by

**Héctor Penagos**

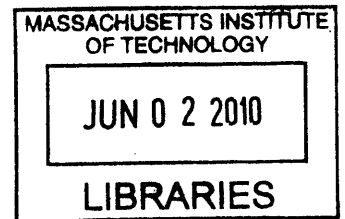
Licenciatura en Física,  
Universidad de las Américas-Puebla, 2000

SUBMITTED TO THE DIVISION OF HEALTH SCIENCES AND TECHNOLOGY  
IN PARTIAL FULFILLMENT OF THE REQUIREMENTS FOR THE DEGREE OF

DOCTOR OF PHILOSOPHY IN HEALTH SCIENCES AND TECHNOLOGY  
AT THE  
MASSACHUSETTS INSTITUTE OF TECHNOLOGY  
JUNE 2010

© 2010 Massachusetts Institute of Technology  
All rights reserved.

**ARCHIVES**



Signature of Author: \_\_\_\_\_

Division of Health Sciences and Technology  
May 14, 2010

Certified by: \_\_\_\_\_

Matthew A. Wilson, Ph. D.  
Sherman Fairchild Professor of Neuroscience  
Picower Institute for Learning and Memory  
Departments of Brain and Cognitive Sciences, and Biology  
Thesis Supervisor

Accepted by: \_\_\_\_\_

Ram Sasisekharan, Ph. D.  
Director, Harvard-MIT Division of Health Sciences and Technology  
Edward Hood Taplin Professor of Health Sciences & Technology and Biological  
Engineering



# Interactions between Anterior Thalamus and Hippocampus during Different Behavioral States in the Rat

by

Héctor Penagos

Submitted to the Division of Health Sciences and Technology  
on May 14, 2010

in partial fulfillment of the requirements for the degree of  
Doctor of Philosophy in Health Sciences and Technology

## ABSTRACT

The anterior thalamus and hippocampus are part of an extended network of brain structures underlying cognitive functions such as episodic memory and spatial navigation. Earlier work in rodents has demonstrated that hippocampal cell ensembles re-express firing profiles associated with previously experienced spatial behavior. Such recapitulation occurs during periods of awake immobility, slow wave sleep (SWS) and rapid eye movement sleep (REM). Despite its close functional and anatomical association with the hippocampus, whether or how activity in the anterior thalamus is related to activity in the hippocampus during behavioral states characterized by hippocampal replay remains unknown.

Here, we monitor and compare thalamic and hippocampal activities during epochs in which rats execute a simple alternation task on a circular maze as well as during sleep periods before and after track running. We employ a neural decoding algorithm to interpret spiking activity in terms of spatial correlates during wake and REM. We analyze multi unit activity (MUA) to characterize the organization of thalamic and hippocampal populations during SWS.

Consistent with their role in spatial navigation, we show that during active locomotion ensembles of thalamic and hippocampal neurons represent the spatial behavior of the rat in a coordinated fashion. However, during periods of hippocampal awake replay their spatial representations become decoupled. During REM, we demonstrate that thalamic activity replicates broad activity patterns associated with awake behavior and that both hippocampus and anterior thalamus concurrently represent similar ambulatory states. During SWS, we establish that the activities in these two areas alternate between frames of elevated firing and periods of little or no activity. We show that there is a tendency for thalamic depolarized states to start and end ahead of hippocampal activity frames.

These results may shed light on how information encoded by thalamic circuits could bias or be incorporated into hippocampal replay phenomena.

Thesis Supervisor: Matthew A. Wilson

Title: Sherman Fairchild Professor of Neuroscience



## **Acknowledgments**

I am grateful to my thesis advisor Matt Wilson for patiently providing me with guidance, for always being available when I needed direction and for all the insights that helped me better understand my data. Through example, Matt has taught me how to be a better scientist. I feel privileged to have worked for someone I deeply admire and respect.

I feel fortunate to have had Jennifer Melcher, Andrew Oxenham and Dennis Freeman as my mentors during my early years in the program. I learned a great deal from their integrity, carefulness, dedication and enthusiasm. I am grateful for the trust they had in me when I worked for them.

I would like to thank the members of my thesis committee, Chris Brown, Dan Merfeld and Sebastian Seung, for their time and helpful feedback.

Working in the Wilson lab was a great experience thanks to the support, encouragement and friendship I received from all my labmates. In particular, I would like to gratefully acknowledge Jun Yamamoto for patiently training me during my initial years in the lab. The quality of my data is, in large part, a direct reflection of all the lessons I learned from Jun.

I feel infinite gratitude for all the love and patience that my wife, Isabel Esquitín, has given me during these years.

Lastly, I would like to thank my parents for their love, encouragement and support.



## TABLE OF CONTENTS

<b>Acknowledgments .....</b>	<b>5</b>
<b>Chapter 1. Introduction .....</b>	<b>9</b>
<b>Chapter 2. Characterization of thalamo-hippocampal interactions during active behavior, awake immobility and slow wave sleep .....</b>	<b>31</b>
<b>Chapter 3. Spatial representations in the rat anterior thalamus and hippocampus during rapid eye movement sleep .....</b>	<b>75</b>
<b>Chapter 4. Summary and Conclusions .....</b>	<b>117</b>
<b>References .....</b>	<b>123</b>



## **Chapter 1**

### **Introduction**

The anterior thalamus and hippocampus are part of a network of brain structures implicated in a range of cognitive functions including episodic memory, navigation and imagination (Kreiman, Koch & Fried 2000; Addis, Wong & Schacter 2007; Byrne, Becker & Burgess 2007; Aggleton 2008; Hasselmo 2009; Vann, Aggleton & Maguire 2009; Buckner 2010). The involvement of these areas in the functions above has been inferred from imaging studies or human clinical data. For instance, bilateral pathology of either thalamus or hippocampus results in the most detrimental cases of anterograde amnesia in humans (Scoville & Milner 2000; der Werf et al. 2003; Josseume et al. 2007). Similarly, patients suffering from memory deficits caused by hippocampal or thalamic damage lack the ability to imagine or plan future events with the abundance of details reported by normal subjects (Hassabis et al. 2007; Kopelman et al. 2009). Functional magnetic resonance imaging (fMRI) studies report consistent activation of the hippocampus when subjects are required to imagine fictitious or future events or during virtual navigation tasks (Ekstrom et al. 2005; Hassabis, Kumaran & Maguire 2007).

Efforts to understand the brain mechanisms that give rise to human cognitive abilities are constrained to the use of noninvasive methods in experiments that directly involve human subjects. Current imaging technologies such as MRI enable us to observe brain areas with unprecedented resolution (Thomas et al. 2008; Hoffmann et al. 2009; Metcalf et al. 2009; Sanchez-Panchuelo et al. 2010). Yet, the smallest volume of brain tissue whose activity level can be measured with imaging techniques lacks adequate temporal and spatial resolution to assess its role in the function or task under investigation. For the

most part, imaging studies are useful in revealing patterns of activation that suggest the participation of brain areas in any given task. In light of these limitations, we turn to animal research.

The rat has been widely favored as a model to study the brain mechanisms underlying spatial navigation and memory. The choice has primarily been driven by the observation that the firing of individual hippocampal neurons is modulated by the position of the animal in space (O'Keefe & Dostrovsky 1971). Place cells are active in restricted locations of an environment and show little or no activity elsewhere. When a rat moves through a trajectory, the sequence in which place cells become active reflects the path traversed by the animal. Thus a connection between a physiological measure and the spatial aspect of an experience is established. Complementing the position coding of place cells, neurons in the rat anterior thalamus are modulated by the orientation of the rat's head relative to the environment (Taube 1995). A given head direction (HD) cell is active within a fraction of orientation space and fires maximally when the rat faces in the cell's preferred direction. It is generally accepted that hippocampal and thalamic cells provide internal representations of position and orientation that could be used for navigation (McNaughton et al. 2006; Whitlock et al. 2008; Calton & Taube 2009).

Despite the extensive functional association between the thalamus and hippocampus, most electrophysiological research efforts in the rat have focused on studying each structure in isolation. This approach has allowed the discovery of remarkable phenomena. For example, during periods in which rats rest, place

cells have been shown to re-express sequences of positions previously visited by the animal (Wilson & McNaughton 1994; Louie & Wilson 2001; Lee & Wilson 2002; Foster & Wilson 2006; Csicsvari et al. 2007; Diba & Buzsáki 2007; Davidson, Kloosterman & Wilson 2009; Karlsson & Frank 2009). The replay of familiar trajectories by hippocampal cells reflects the memory of an event. Whether thalamic cells express similar reactivation patterns is unknown. More generally, how activities in the hippocampus and thalamus influence one another remains, for the most part, an open question. In this work, we take a step towards expanding our understanding of how these areas interact by simultaneously monitoring their activities in the freely behaving rat. Specifically, we record place cells in the CA1 layer of the dorsal hippocampus and of HD cells in the dorsal division of the anterior thalamic complex. We characterize the neuronal activity at the individual, ensemble and population levels during active behavior and natural sleep.

To provide context for the present work, in what follows I briefly summarize previous research related to the anatomy and electrophysiology of the anterior thalamus and hippocampus.

## **Anatomy**

Papez (1937) described an anatomical loop that started and ended in the hippocampal formation and included the mammillary bodies, anterior thalamus, and retrosplenial cortex. The anatomical connections among these structures are, except for one case, reciprocal. In general, the pattern of connections is as

follows: projections from the anterior thalamus reach the hippocampus in two steps. They first synapse onto cells of the subicular complex and then project to the entorhinal cortex, which provides the majority of inputs to the hippocampus. The output of the hippocampus is carried by a fiber bundle known as the fornix which synapses onto the anterior thalamus and the mammillary bodies. Completing the loop, the mammillary bodies project to the anterior thalamus via the mamillothalamic tract. No reciprocal connections are sent from the thalamus to the mammillary nucleus. An additional route for communication between the anterior thalamus and hippocampus is provided by the retrosplenial cortex, which is reciprocally connected with both areas.

Broadly speaking, the thalamus has two organization principles common to all its constituent regions: first, thalamic nuclei are reciprocally connected with their cortical targets and, second, while inhibition can be mediated by local interneurons, the bulk of inhibition is provided by cells from the thalamic reticular formation (Jones 2007). In general, as thalamocortical cells project to cortex, they send axon collaterals to reticular formation inhibitory interneurons. Similarly, corticothalamic cells projecting back onto thalamocortical cells send axon collaterals to reticular neurons. Both thalamocortical and corticothalamic neurons use glutamate as a neurotransmitter and have an excitatory effect on their targets. By contrast, reticular cells use the neurotransmitter gamma-aminobutyric acid (GABA) and have an inhibitory effect. Some studies suggest that reticular cells project back to the same thalamocortical cells innervating them, keeping a high degree of specificity in their connections.

The anterior thalamic complex is divided into ventral, medial and dorsal nuclei. Each nucleus receives a different pattern of innervation from the mammillary bodies. The dorsal nucleus receives inputs from the lateral division, while medial and ventral nuclei receive inputs from the medial aspect of the mammillary bodies (Vann & Aggleton 2004). At least in the macaque monkey, projections to medial and ventral nuclei arise in distinct areas within the medial mammillary nucleus (Vann, Saunders & Aggleton 2007). Cells from the three anterior thalamic divisions are considered to be mainly projection cells. In the rat, inhibition to the anterior thalamus has been shown to come exclusively from neurons of the thalamic reticular formation. However, in the cat, there exist reports that the anterior thalamus is devoid of reticular innervation and inhibition is thought to be carried by local interneurons (Paré, Dossi & Steriade 1991).

About 60% of neurons recorded in the dorsal thalamic nucleus have been reported to be HD modulated (Taube 1995). Neurons in the remaining anterior nuclei are not spatially tuned. Instead, a large fraction of cells fire rhythmically in the theta frequency (see below). Given the difference in innervation and activity patterns displayed by cells in each nucleus, it has been proposed that each division of the anterior thalamus is involved in different functions (Vann & Aggleton 2004).

The hippocampal formation encompasses several structures from the medial temporal lobe: the hippocampus proper (subfields CA1, CA2 and CA3), dentate gyrus, subicular complex and entorhinal cortex (Andersen 2007). Information flow in the hippocampal formation is mainly unidirectional. The major excitatory

circuits of the hippocampal formation are as follows: Axons from layers II and III of the entorhinal cortex form a fiber bundle known as the perforant pathway. Axons originating in layer III synapse onto CA1 and subicular cells. Axons from layer II project to granule cells in the dentate gyrus and pyramidal cells in CA1. Cells in dentate gyrus project to CA3 via mossy fibers. In turn, CA3 pyramidal cells send projections to CA1 cells via Schaffer collaterals. CA1 cells synapse on subicular cells. Closing the loop initiated in the entorhinal cortex, both CA1 and subicular cells project to the deep layers of the entorhinal cortex. In addition to the excitatory loops, inhibition is provided by a wide variety of local interneurons (Klausberger et al. 2003; Klausberger & Somogyi 2008). Cells from all subfields of the hippocampus fire rhythmically in the theta range and display a strong spatial modulation.

### **Spatial Correlates**

An ubiquitous feature in this network of structures is the presence of neurons whose activity is strongly correlated with the spatial behavior of the rat. Place cells have been identified in all the structures of the hippocampal formation and are also found in the retrosplenial cortex (McNaughton, Barnes & O'Keefe 1983; Rose, Diamond & Lynch 1983; Sharp & Green 1994; Cho & Sharp 2001; Fyhn et al. 2004). By contrast, HD cells are primarily found in the extrahippocampal components of the circuit: lateral mammillary bodies, posterior cingulate cortex, post-subiculum and entorhinal cortex (Taube, Muller & Ranck 1990; Taube 1995; Sharp 1996; Stackman & Taube 1998). Neurons that reflect a combination of position and orientation information are found in the subicular complex as well

as retrosplenial and entorhinal cortices (Fyhn et al. 2008).

The spatially modulated activities of place and HD cells have been extensively studied. However, the exact mechanisms that give rise to their complex firing properties are not fully understood. In what follows, I will briefly outline what is known about the generation of thalamic directional signals.

Broadly speaking, thalamic HD firing is hypothesized to arise from the integration of allothetic (environmental features) and ideothetic (self-generated) information. The influence of allothetic information is best illustrated by the strong control exerted by salient visual landmarks on the directional tuning of HD cells. For example, when rats are placed in a cylindrical environment that contains a single contrasting cue card attached to the wall, the directional preference of HD cells become coupled to the location of the card (Taube, Muller & Ranck 1990). If the card is rotated, the preferred direction of individual cells rotate by a similar angle. The effect is more robust if the card rotation is done when the rat is not in the recording arena. However, for familiar environments, card rotations in the presence of the animal can still induce the shift of the firing preferences. Given the direct connection between visual cortical areas and the retrosplenial cortex and subiculum, these latter areas are thought to incorporate allothetic information to the extended circuit of HD cells.

The ideothetic components that gives rise to the directional tuning of thalamic cells are thought to arise from vestibular and motor related signals. The fundamental role played by vestibular input in the generation of directional signals has been demonstrated by experiments in which the reversible inactivation of the vestibular organs in the inner ear abolish the directional firing of HD cells (Stackman & Taube 1997). Importantly, directional tuning returns in

a timescale that mirrors the recovery of vestibular function. The integration of angular velocity information generated in vestibular organs has been postulated as a mechanism for the generation of the orientation signal (Stackman & Taube 1998). Notably, signals related to the motor behavior of the rat are also known to be necessary for the generation of HD cell firing. Passive rotations of restrained rats abolish directional firing (Stackman et al. 2003).

What is the relative contribution of allothetic and ideothetic information in the generation of directional firing? Available data points to ideothetic information as the source of directional firing and allothetic information as a mechanism to correct the accumulation of errors in the integration of angular velocity information (Knierim, Kudrimoti & McNaughton 1998). This notion is further strengthened by the findings that lesions to either the postsubiculum or retrosplenial cortex do not abolish the directional firing of thalamic HD cells (Goodridge & Taube 1997). However, cells in lesioned animals exhibit unstable firing with substantial drift in their preferred directions over several minutes.

What gives rise to the spatial tuning of place cells? A complete answer to this question is difficult given the convergence of high-level sensory information onto the hippocampus. This is illustrated by the findings that geometrical modifications of the recording environment, manipulations of spatial cues or changes in behavioral demands tend to introduce alterations in the firing of place cells (Markus et al. 1995; Leutgeb et al. 2005a, b). Some of these changes are manifested as modifications in firing rates without alterations in the location of the cell's receptive field. Other manipulations result in the complete silencing of a cell or the emergence of a new receptive field. How geometrical, sensory,

mnemonic or motivational informations are integrated to generate place field firing is unknown. Despite the above limitations, progress has been made in understanding how spatial information from other brain areas give rise to the location specificity of place cells (Solstad, Moser & Einevoll 2006). In particular, the discovery of spatially modulated cells in the medial entorhinal cortex (MEC) has prompted models that integrate this information to produce hippocampal place cell firing . Principal cells in MEC fire with spatial periodicity as rats explore an environment. Given their remarkable regular firing, these neurons are referred to as grid cells. Grid cells are active in all environments and the spacing between adjacent firing fields increases progressively from the dorsal to ventral aspects of MEC. Linear combinations of grid cells with varying field spacing, along with directional information, have been successfully modeled to result in single peaked place cells.

Are the activities of hippocampal place cells and thalamic HD cells related? Some studies indicate several instances in which place and HD cells act in a coordinated manner and share similar input dependencies. For example, both cell types have been shown to be heavily dependent on an intact vestibular system (Stackman, Clark & Taube 2002). Just like HD cells loose their orientation tuning, place cell firing is altered during vestibular inactivation experiments. Similarly, the re-orienting effect that salient visual cues have on HD cells is also manifested by similar rotations of the receptive fields of place cell ensembles (Knierim, Kudrimoti & McNaughton 1998). It is important to note that not all manipulations result in a coordinated shift in the spatial tuning of HD and place cell systems. For example, when a cue card is rotated to produce a conflict with

other available cues, place cells will either rotate in register with HD cells or express different location preferences altogether.

## **Sleep electrophysiology**

### *Hippocampus*

The hippocampus displays striking differences in activity as a function of vigilance state, primarily at the collective cell level. Pyramidal cells from the CA1 subfield of the hippocampus tend to fire bursts of 2-3 spikes, each with decreasing amplitude, during wake. This firing pattern is known as complex spike bursting (McNaughton, Barnes & O'Keefe 1983). During active locomotion, pyramidal cells produce complex spike bursts in a rhythmic fashion. As a consequence, the aggregate multi unit activity (MUA) displays a periodic modulation. The frequency range that characterizes this recurrent pattern lies within the theta (6 - 10 Hz) band. Not surprisingly, the local field potential (lfp) is also dominated by activity in the same frequency range (Vertes, Hoover & Prisco 2004).

Complex bursting remains prevalent during sleep. In addition, during rapid eye movement sleep (REM) hippocampal activity continues to show rhythmic modulation in the theta band, which constitutes the hallmark of hippocampal activity during REM. By contrast, noticeable differences in the population activity patterns arise during the sleep stage known as slow wave sleep (SWS). Instead of exhibiting a continually varying level of activity, MUA displays discrete, large amplitude bursts embedded in a relatively quiet activity

background. These bursts arise from the recruitment of large numbers of pyramidal cells and are accompanied by distinct oscillatory patterns in the lfp, known as sharp wave - ripple (SPW-R) events (Buzsáki, Leung & Vanderwolf 1983). SPW-Rs consist of the superposition of a 100 - 300 Hz oscillation over a slower deflection in the lfp trace. Contrary to the variable duration exhibited by MUA bursts, SPW-Rs appear to last 50 - 100 ms giving rise to the possibility that series of SPW-Rs might be chained into trains of variable time length (Davidson, Kloosterman & Wilson 2009).

The mechanisms that give rise to individual SPW-Rs are only partially understood. The sharp wave component is thought to reflect synaptic activity that arises from highly synchronous firing of CA3 cells synapsing onto CA1 neurons (Buzsáki 1989). Although ripples are thought to reflect rhythmic inhibition on CA1 pyramidal cells, how quick oscillating inhibition is achieved is unclear. For example, firing of the interneuron population during ripple activity is significantly increased, consistent with their hypothesized participation in the oscillation (Klausberger et al. 2003). However, extracellular recordings fail to detect rhythmic spiking of individual interneurons (Csicsvari et al. 1998; Csicsvari et al. 1999). These observations suggest ripple activity might be the result of complex interactions of networks of inhibitory cells rather than the simple reflection of their intrinsic cellular properties. It is well established that hippocampal interneurons exert their inhibitory effects through the neurotransmitter GABA at chemical synapses. Interestingly, blockade of GABA<sub>A</sub> receptors in slices does not abolish ripples (Maier, Nimrich & Draguhn 2003). This finding has led to the proposal that electrical coupling among CA1 neurons might serve as an additional element to sustain ripple oscillations. However, the

actual involvement of electrical signaling, mediated by gap junctions, remains to be determined. Data from studies in connexin 36 knock-out mice, which lack the gene that codes for neuron-specific gap junctions, are controversial. A study in hippocampal slices from knock-out mice reported fewer spontaneous SPW-Rs than those produced in slices from littermate controls (Maier et al. 2002). By contrast, a report from *in vivo* recordings found no statistical difference in ripple features such as occurrence rate, power or frequency between wild type and knockout mice (Buhl et al. 2003). It is important to point out that SPW-Rs are not an exclusive feature of SWS. They are also observed during periods of immobility as rats pause during active exploratory behavior.

Recent observations have revealed a broader organization principle of hippocampal MUA and lfp during SWS. Population activity exhibits periods of sharp increases in firing rate flanked by epochs of little or no firing (Wolansky et al. 2006; Ji & Wilson 2007). This pattern is strongly reminiscent of the slow oscillation, with its corresponding up/down states, previously found in intracellular recordings in the neocortex. Interestingly, cortical and hippocampal slow oscillations appear to be transiently correlated. Note that the starting phase of the hippocampal up state tends to coincide with the occurrence of SPW-Rs and, in general, it encompasses several MUA bursts. The mechanisms that give rise to the hippocampal oscillation are still unknown. However, similar to the cortical oscillation, an important factor that seems to modulate the appearance of the up/down alternation is the the state of the brainstem cholinergic pathway.

The relevance of hippocampal activity during sleep arises from the hypothesized

function this state might hold for the process of memory consolidation. An influential theory proposes the existence of two stages in the establishment of a memory: an initial phase in which mnemonic information is temporarily stored in the hippocampus, followed by its relocation to neocortical sites for long term storage (Buzsáki 1989). A proposal from this theory is that offline states such as sleep provide an ideal stage for memory consolidation. The process of information transfer has been postulated to involve the broadcast of patterns of activity that represent prior experiences by hippocampal cells. Consistent with this notion, several studies have reported the activation of sets of place cells in an experience dependent manner during SPW-Rs occurring in SWS. In one report, pairs of neurons with overlapping place fields were shown to increase correlated spiking during SPW-Rs in sleep following exploration of a rectangular arena (Wilson & McNaughton 1994). Another study found that the tendency of cells to be co-active during SPW-Rs was directly related to the number of times rats visited the cell's receptive field during awake behavior (O'Neill et al. 2008). In a study looking at sets of at least three neurons, place cells were found to re-express the sequential order in which they were active during exploration of a linear maze (Lee & Wilson 2002). These findings are consistent with the notion that the hippocampus may transmit information during SWS. What do cortical areas, presumably at the receiving end of this communication loop, do during such reactivation events? Two studies have demonstrated interactions between cortex and hippocampus during SWS. In one report, ripples were found to be correlated with oscillatory events in the medial prefrontal cortex (Siapas & Wilson 1998). Specifically, ripples tended to occur just prior to cortical spindles (7 - 14 Hz oscillations, see below). This finding highlights the possibility that

hippocampal activity could bias the selection of cortical neurons that are active in spindle oscillations. A conceivable consequence would be the strengthening of the representation encoded by the selected cortical neurons.

In a recent study, the correlation between cortical and hippocampal up states during SWS was assessed (Ji & Wilson 2007). Analysis at the population level revealed that increased population activity in the visual cortex tended to start roughly 50 ms before the initiation of the corresponding hippocampal up state. Interestingly, frames of elevated activity in which cell ensembles in each brain area replayed trajectories previously expressed during exploration tended to overlap in time. In addition, time intervals between pairs of cells, each belonging to a different area, measured during up states were correlated with the corresponding time intervals during behavior. This study further strengthens the possibility that the organization of brain activity in frames during SWS might provide time windows during which cortical and hippocampal units become coordinated at a fine temporal scale to support memory consolidation processes.

Importantly, recapitulation of awake hippocampal activity in the rat brain has also been identified during REM (Louie & Wilson 2001). Several differences exist relative to the hippocampal patterns expressed during SWS. Ensemble reactivation during REM tends to happen several hours after rats run on the track, with most matches being identified 24 hours following exposure to the maze. In addition, REM replay patterns last tens of seconds matching the duration of the rat's behavioral experience. By contrast, SWS replay events are compressed 10 to 20-fold relative to the awake trajectories they represent. An important aspect of REM replay is the possibility that the reported hippocampal

reactivation might be part of a more extensive recapitulation of the awake state. Note that the theta oscillation that characterizes both the awake locomotive state and REM, is influenced by activity of brainstem nuclei. Because during ensemble replay theta modulation displays a high degree of similarity to the corresponding awake experience, it seems plausible that other brain areas might also be engaged during REM replay.

### *Thalamus*

The differences in thalamic patterns of activity that characterize the sleep and wake states are manifested both at the individual cell and population levels. During wake and REM, thalamocortical cells display a tonic firing mode in which series of individual action potentials are fired when cells reach a threshold level of depolarization. By contrast, during SWS thalamic neurons predominantly fire bursts of action potentials. What mechanisms give rise to the differences in firing modality? Part of the answer lies in the fact that several neurotransmitter pathways, which exert a modulatory function on thalamic cells, display distinct activity profiles during wake and sleep (Hobson & Pace-Schott 2002; Pace-Schott & Hobson 2002). These modulatory systems include acetylcholine, glutamate, serotonin and norepinephrine. Their nuclei are located in the brainstem and have widespread connections in the thalamus and cortex. To illustrate the effect the above modulatory systems have on thalamic cells, consider the cholinergic pathway (Steriade 2004). Cholinergic cells project to both thalamocortical and reticular thalamic neurons with opposite effects on each cell type: they excite thalamocortical cells and inhibit reticular neurons. During wake, cholinergic

neurons have an elevated level of activity. As a consequence, thalamocortical cells become more excitable because of the aggregate effect of direct excitation by brainstem neurons and diminished inhibition from reticular cells. By contrast, during SWS, brainstem cholinergic neurons decrease their activity level. Consequently, excitatory drive on thalamocortical cells and inhibition on reticular neurons are both greatly reduced. The net result is a deep hyperpolarization of thalamocortical cells. Burst firing arises from the effect that such prolonged hyperpolarization periods have on T type  $\text{Ca}^{2+}$  channels, which are expressed at the soma and dendrites of thalamic cells (Bal, von Krosigk & McCormick 1995). T channels can be activated or inactivated depending on the state of two voltage sensitive gates. Both gates are open if the cell is slightly depolarized after a long period of hyperpolarization. The activation of the channel results in a low threshold  $\text{Ca}^{2+}$  spike which depolarizes the cell to a sufficiently high level to produce conventional action potentials. Because inactivation of the T channels is slow, the cell depolarization level is maintained for about 50 - 200 ms, which results in the generation of several action potentials in quick succession. Note that if the cell membrane is maintained within a relatively depolarized level for sufficiently long intervals, T channels are inactivated and the cell is only able to generate conventional spikes. Therefore, T channels grant thalamic cells the ability to display different firing modalities as a function of the recent history of their membrane potentials.

A typical feature of thalamic population activity during SWS is the periodicity with which it occurs. The most prominent rhythms readily apparent in the thalamic lfp are the slow (0.3 - 1 Hz), delta (1 - 4 Hz) and spindle (7 - 14 Hz)

oscillations (Steriade, Nuñez & Amzica 1993). Delta waves are thought to reflect the intrinsic propensity for individual cells to emit bursts in a cyclic fashion. This tendency arises from the interaction between low threshold  $\text{Ca}^{2+}$  currents and a cation current known as the h current (McCormick & Pape 1990). The h current is activated at more negative potentials than the  $\text{Ca}^{2+}$  current and has a reversal potential around -35 mV. After extended periods of hyperpolarization, the h current promotes a slow depolarization of thalamic cells that leads to the activation of T channels. What follows is the generation of a low threshold  $\text{Ca}^{2+}$  spike and associated burst of action potentials. On the falling phase of the  $\text{Ca}^{2+}$  spike, the inactivation of T channels and deactivation of the h current results in a hyperpolarization overshoot that leads to the activation of the h current and the start of a new burst cycle with another  $\text{Ca}^{2+}$  spike. This regenerative process takes place with a periodicity in the 1 - 4 Hz range and is most prevalent during the deeper stages of SWS.

The onset of sleep is characterized by spindle oscillations; sharp deflections in the lfp with a 7 - 14 Hz repetition rate occurring in epochs lasting 1 - 3 seconds and recurring every 3 - 15 seconds. Several lines of evidence from *in vitro* and *in vivo* studies support the proposal that spindle oscillations arise from reciprocal synaptic interactions between thalamocortical and thalamic reticular cells (Steriade, Nuñez & Amzica 1993). For instance, preparations in which reticular input is selectively removed, thalamocortical cells fail to generate spindles (Steriade et al. 1985). Additionally, intracellular recordings in reticular neurons have shown the emergence of feedback excitatory post synaptic potentials (EPSPs) in phase with thalamocortical bursts (Destexhe, McCormick & Sejnowski 1993). These EPSPs appear roughly 100 ms after applying electrical

stimulation to reticular cells. The timing is consistent with reticular neurons exerting a sufficiently strong inhibition on thalamocortical cells to produce low threshold  $\text{Ca}^{2+}$  spikes along with bursting activity, which then results in reticular EPSPs.

The 7 - 14 Hz frequency range that characterizes spindle oscillations is thought to emerge from the combination of the timing in reciprocal synaptic events between reticular and thalamocortical cells, and from intrinsic burst firing properties of reticular neurons. The slow recurrence of spindles every 5 - 15 seconds is ascribed to the incremental depolarization of thalamocortical cells during the generation of spindles. The depolarization renders thalamocortical cells refractory by preventing a fast activation of the h current and by diminishing the hyperpolarizing effects of reticular cells. Both effects inhibit the generation of low threshold spikes and prevent additional cycles from being generated.

The third rhythm that modulates thalamic activity during SWS is the slow oscillation. Unlike delta and spindle waves, the slow oscillation is generated in cortex and imposed onto thalamic cells via corticothalamic projections (Steriade et al. 1993). The slow oscillation correspond to the alternation in activity levels in cortex (up/down states) and is reflected as a slow depolarization envelope in the thalamic lfp. The slow oscillation groups all sleep rhythms generated in the thalamus in discrete epochs of complex oscillatory activity. Each discrete event is characterized by the expression of spindles at the onset of the depolarization, followed by delta oscillations until the termination of the cortical up state.

What are the implications of the patterns of activity exhibited by thalamic cells

during sleep? The change from tonic to burst firing between wake and SWS has been interpreted to reflect the ability of thalamic cells to differentially gate incoming sensory information during distinct behavioral states. This function is supported because, by firing in a periodic fashion during SWS, thalamic activity is decoupled from sensory drive. Besides its role in disconnecting the brain from external stimuli, it is possible that the thalamus might contribute in other functions during sleep. Consider, for example, the case of spindle oscillations. It has been suggested that cortical spindles might provide a window of opportunity for hippocampus and cortex to interact in the consolidation of hippocampus-dependent memories (Siapas & Wilson 1998). Importantly, spindles are associated with increases in intracellular  $Ca^{2+}$  concentrations that may facilitate plasticity mechanisms in cortical neurons. As discussed above, spindles are generated in the thalamus and synaptically imposed on cortical neurons. It is conceivable that thalamic activity might contribute to coordinate cortico-hippocampal interactions by biasing the time of spindle occurrence to coincide with that of hippocampal ripples.

REM provides another state for potential thalamic participation in sleep processes. Our current understanding of thalamic physiology indicates that, during REM, corticothalamic cells have the ability to display tonic firing. A potential consequence is that, at the ensemble level, thalamic cells may resemble activity profiles expressed during awake behavior. Such activity could contribute to the rich sensory content that characterizes the dreaming state and is one of the possibilities we explore in this thesis.

## **Chapter outline**

Each chapter in this thesis is prepared to be a self-contained piece of work. Some overlap between chapters is unavoidable.

In chapter 2, we explore the spatial representations encoded by ensembles of hippocampal and thalamic cells during active locomotion and periods of stationary behavior. We specifically ask whether thalamic representation of orientation is maintained in register with hippocampal representation of location during trajectory replay in awake immobility. In addition, during SWS, we investigate the organization of population activity in both brain areas and assess their interactions through measures of correlation.

In chapter 3, we examine the ensemble activity of thalamic HD cells during REM sleep. We ask whether a temporal structure exists in the observed spiking patterns and assess their relation to the firing profiles displayed during awake behavior. We also compare the orientation trajectories represented by HD and place cells during REM sleep to investigate what features of awake behavior are encoded by thalamus and hippocampus.

In chapter 4, a summary of our observations and a brief conclusion is presented.



## **Chapter 2**

### **Characterization of thalamo-hippocampal interactions during active behavior, awake immobility and slow wave sleep**

## **Introduction**

The rodent anterior thalamus and hippocampus have been studied extensively as a model to understand the mechanisms underlying spatial memory and navigation. Anatomically, these structures share direct reciprocal connections as well as indirect means of communication through the retrosplenial cortex and mammillary bodies (Papez 1937). Consistent with their role in spatial navigation, neurons in the hippocampus and anterior thalamus display robust spatial correlates in their discharge properties. Hippocampal pyramidal cells, place cells, fire in restricted regions of space reflecting the current location of the animal (O'Keefe & Dostrovsky 1971). Neurons from the dorsal nucleus of the anterior thalamus (ADN) discharge as a function of the orientation of the animal's head in the environment (Taube 1995). These cells are referred to as head direction (HD) cells. The activities of place and HD cells are thought to form internal representations of location and direction, respectively. Given their complementary spatial information content, HD and place cells are expected to act in a synergistic fashion during navigation (McNaughton et al. 2006; Whitlock et al. 2008; Calton & Taube 2009). Reinforcing the notion of cooperative activity between the hippocampus and ADN, lesion studies have demonstrated similar deficits in spatial memory tasks when either structure is compromised. Performance is impaired in alternation tasks on the T maze, radial arm maze or in a spatial reference version of the water maze (Aggleton et al. 1995; Warburton & Aggleton 1999; Warburton et al. 2000). In addition, electrophysiological experiments demonstrate that manipulations that change the preferred orientation of HD cells have a comparable reorienting effect on the

receptive fields of place cells (Knierim, Kudrimoti & McNaughton 1998). Similarly, interventions that disrupt the firing selectivity of thalamic HD cells tend to also alter the spatial tuning of place cells and ultimately have a detrimental effect in navigation (Brown, Yates & Taube 2002; Stackman, Clark & Taube 2002; Yoder & Taube 2009).

Notably, besides reflecting the animal's current location, place cell ensembles have been shown to fire in a sequential manner during brief bursts of multi unit activity (MUA) as rats pause during navigation (Foster & Wilson 2006; Csicsvari et al. 2007; Diba & Buzsáki 2007; Davidson, Kloosterman & Wilson 2009; Karlsson & Frank 2009; Gupta et al. 2010). Because in initial reports it was shown that these firing patterns represented trajectories rats had previously experienced, they were referred to as replay events. Given the complementary spatial representation provided by HD cells and their anatomical relation to the hippocampus, a question that arises is whether HD neurons express similar replay activity.

Note that hippocampal replay has also been identified throughout slow wave sleep (SWS) during MUA bursts embedded within broader increases in population activity (Wilson & McNaughton 1994; Lee & Wilson 2002; O'Neill et al. 2008). The periodic alternations in hippocampal state appear to provide periods for communication between the hippocampus and other brain areas during SWS. In particular, cortical up states have been shown to be correlated with similar hippocampal up states (Ji & Wilson 2007). Because thalamic neurons have been shown to also exhibit up-down activity modulations, here we ask whether a relationship exists between the ADN and hippocampus during such sleep states.

To address the questions above, we sought to determine the degree of coordinated activity between the hippocampus and ADN during different behavioral states in the rat. To this end, we simultaneously monitored the activity of groups of thalamic HD cells and place cells in the CA1 layer of the dorsal hippocampus. We report that during active locomotion, spiking patterns in both areas faithfully reflect the spatial behavior of the animal. By contrast, during pauses in exploration HD cells reflect the animal's current orientation while place cells represent partial track traversals in a time compressed manner. During SWS, we characterize hippocampal and thalamic activities at the population level. We demonstrate that a timing relationship exists between thalamic and hippocampal up-states as well as between bursts of MUA in the two areas. These results suggest a continued interaction during sleep.

## **Results**

Figures 1 and 2 show representative locations of thalamic and hippocampal recording sites for one rat. HD and place cells were recorded from four rats during exploration of a circular track and during sleep before (PRE) and after (POST) maze running (RUN). Only units that were unambiguously isolated during sleep and active behavior were used in the analysis. Additionally, we only included place cells that had mean firing rates above 0.2 Hz. All HD cells were used in the analysis. Figure 3A and B show the spiking activity of representative HD and place cells during maze exploration as one rat ran back and forth between two points separated by a high wall divider for food reward. Figures 3C and D display the receptive fields of the sample of HD and place cells for the

same rat. Note that, to simplify the analysis, location information (such as place fields) was expressed on linear coordinates representing the distance to one of the food wells (see Methods).

### *Representation of spatial behavior during wake*

Successful navigation requires the integration of information about the animal's location and heading direction. We tested the notion that place and HD cells provide a coordinated internal representation of the rat's spatial behavior during exploration. To this end, we used a neural decoding algorithm to interpret the activity of place and HD cells in terms of the rat's position and head orientation (Zhang et al. 1998; Johnson, Seeland & Redish 2005). Decoding allows to estimate the likelihood with which the rat occupies a particular position, or is oriented in a particular direction, given the ensemble firing profile displayed in an observation window of arbitrary duration. We employed a 250 ms decoding window. The output of the estimation algorithm is a probability density function (PDF) over position or orientation. Thalamic (HD) cells were used to estimate heading direction, while hippocampal (place) cells were used to decode both location and orientation. We were able to decode both spatial variables from place cells because, on linear tracks, their firing activities can jointly represent location and running direction (McNaughton, Barnes & O'Keefe 1983; Markus et al. 1995; Battaglia, Sutherland & McNaughton 2004). Figure 4A shows heading direction estimations (white,  $p=0$ ; black,  $p=1$ ) based on the spiking activity of seven HD cells, along with thalamic MUA, during a 120 s interval for one rat. Figure 4B displays orientation and position estimations based on hippocampal

ensemble activity (36 place cells). The corresponding MUA during the same time window is also displayed. This epoch included both periods of active locomotion and immobility as the rat traversed the track during one lap. While heading predictions based on thalamic activity were mostly in line with the rat's true orientation, there were times (primarily stopping segments) during which hippocampal-based estimation differed from the rat's observed spatial behavior. Figure 4C-D provides a closer look at the qualitative difference in estimation accuracy between periods of active locomotion and immobility for both brain regions. Decoding based on thalamic activity faithfully reflected the animal's head orientation irrespective of ambulatory state. By contrast, hippocampal-based estimations consistently worsened during stationary behavior. To quantify these observations, we calculated estimation errors as the difference between the mean value of the observed spatial variable and the estimated value with maximum likelihood in each decoding bin. Figure 4E shows the distribution of aggregate orientation estimation errors as a function of ambulatory state. Estimations were based on HD cells from four rats over eight recording sessions. Median estimation errors were well within the estimation resolution in both conditions (locomotion, 8.62°; stationary, 8.83°). Figure 4 F-G shows the aggregate orientation (F) or position (G) estimation error based on place cell activity. Data includes estimations from three rats over six recording sessions (the number and tuning of place cells was inadequate for spatial estimation in one session for two rats and were excluded from this calculation). Decoding errors were significantly greater during immobility than during locomotion for both orientation (locomotion, mean 26.55°, median 8.84°; stationary, mean 78.11°, median 69.47°,  $P < 0.001$ , rank-sum test) and position (locomotion,

mean 27.67 cm, median 6.32 cm; stationary, mean 128.07 cm, median 55.42 cm;  $P < 0.001$ , rank-sum test) estimations.

### *HD and place cell activity during immobility periods*

In earlier work, Bayesian decoding was successfully used at 20 ms resolution during periods of immobility (Davidson, Kloosterman & Wilson 2009). It was demonstrated that place cell activity is structured to replay partial track traversals at timescales 15-20 times faster than actual behavior. Here we asked whether, during hippocampal replay events, HD cells concurrently represented orientation trajectories that reflected the correlation between position and heading direction observed during actual running behavior. To address this question, we first identified periods of elevated MUA (80 ms minimum duration) occurring while rats paused on the track. We decoded hippocampal spiking activity (20 ms bin) and found the linear path that maximized the mean estimated position likelihood. This served as a score associated with the trajectory and was used to assess the statistical significance of the replay event. Any given trajectory score was compared to distributions of scores obtained after subjecting the original spike data to three different shuffling procedures (Davidson, Kloosterman & Wilson 2009) (see Methods). Decoded trajectories with Monte Carlo p-values  $< 0.05$  defined our set of hippocampal replay events ( $n = 319$ ). We decoded the orientation content from the activity of thalamic HD cells (20 ms resolution) during the epochs spanned by each element of the hippocampal replay set. Figure 5A shows examples of the decoded orientation activity during hippocampal replay events from three different rats. In all

analyzed events, estimations based on hippocampal activity consistently deviated from the rat's current position or head orientation which resulted in large estimation errors (position, mean 131.69 cm, median 73.95 cm; head direction, mean 89.11°, median 89.53°). By contrast, thalamic cells continued to be in register with the rat's current heading despite the use of a short estimation window. The correspondence between estimated and observed orientations was reflected as a significantly lower estimation errors (HD cell-based decoding, mean 51.33°, median 30.84°; place cell-based decoding, mean 89.11°, median 89.53°;  $P < 0.001$ , rank sum test).

#### *Firing mode as a function of behavioral state*

We were also interested in characterizing the firing mode exhibited by place and HD cells as a function of vigilance state. Figure 6 shows 2-D inter spike interval (ISI) and autocorrelation plots for typical HD and place cells during RUN, SWS and rapid eye movement sleep (REM). Each point on a 2-D ISI plot represents the ISIs between a spike and its immediate neighbors, and their clustering profiles provide information about the firing modality exhibited by a cell. A single cluster on a 2-D ISI plot is consistent with a predominantly tonic firing mode. Burst firing gives rise to several clusters on the graph. The lower left cluster is composed of spikes occurring within a burst whereas the lower right and upper left clusters contain spikes at the beginning and end of a burst, respectively. The upper right cluster reflects isolated spikes. Place cells exhibited burst firing across all behavioral states. By contrast, HD cells fired in bursts during SWS only. To quantify this observation, we calculated the degree

of bursting exhibited by each cell type during RUN, SWS and REM. Bursts were defined as sets of spikes with ISIs shorter than 5 ms and whose first spike was preceded by a period of no activity lasting at least 100 ms. The burst index was defined as the percentage of spikes fired during bursts relative to the total number of spikes during a given interval (Ramcharan, Gnadt & Sherman 2005). HD cells tended to have low bursting indices during RUN indicating a predominantly tonic firing mode. During SWS, bursting activity in thalamic cells increased by about one order of magnitude relative to RUN (SWS, mean 2.14 %, median 1.32 %; RUN, mean 0.46 %, median 0.37 %;  $P = 0.005$ , rank-sum test). The tendency for place cells to fire in bursts also increased during SWS (SWS, mean 4.82 %, median 4.01 %; RUN, mean 3.66 %, median 3.18 %;  $P = 0.005$ , rank-sum test). Consistent with previous findings theta modulation was prevalent in hippocampal cells during RUN and REM, but not SWS. HD cells were not theta modulated regardless of behavioral state.

#### *Multi Unit Activity and spatial coding during SWS*

In light of the tendency for HD and place cells to fire in bursts during SWS, we assessed whether a relationship existed between MUA in the thalamus and hippocampus. Figure 7B (left) displays the average cross-correlogram between thalamic and hippocampal MUA during SWS which was calculated with data from four rats spanning a total of 18 sleep sessions. There was a significant correlation between thalamic and hippocampal MUA at both 95 ms ( $P = 0.0026$ , t-test) and -85 ms ( $P < 0.001$ ) time lags. Closer inspection revealed that, consistent with the off-center peaks in the cross-correlogram, hippocampal

bursts tended to be surrounded by elevated thalamic MUA. Note that a single hippocampal burst could be anticipated or followed by high thalamic MUA discharges. The timing between bursts across areas was variable as reflected by the broad peaks in the cross-correlograms in Figure 7B. The fact that bouts of hippocampal elevated MUA were flanked by thalamic bursts within 100 ms is suggestive of reciprocal communication between the two areas.

Next, we tested if, with our extracellular data, thalamic and hippocampal population activity exhibited the periodic alternation between depolarized and hyperpolarized states that characterize the thalamocortical and hippocampal slow oscillations. Consistent with previous studies, we found that both areas exhibited periods of silent activity alternating with epochs of elevated firing (Figure 7A). On average, thalamic depolarized states occurred at a rate of  $45.87 \pm 5.04$  per min (mean  $\pm$  s.e.m.) during SWS ( $n = 49,182$  during 16 sleep sessions from four rats). There was no difference in occurrence rate between PRE and POST (PRE,  $42.14 \pm 8.68$  per min; POST,  $49.60 \pm 5.47$  per min;  $P = 0.479$ , t-test). The duration of the depolarized states varied between 0.1 and 3.5 s in both structures. There was a tendency for thalamic depolarized states to have exhibit longer durations during POST (PRE, mean 0.575 s, median 0.355 s; POST, mean 0.847, median 0.49,  $P < 0.001$ , rank-sum test), with a slight reduction in firing rate per tetrode (PRE, mean 28.98 Hz, median 26.93 Hz; POST, mean 27.53 Hz, median 25.71 Hz;  $P < 0.001$ , rank-sum test). At the same time, the periods of inactivity between thalamic frames tended to be slightly, but significantly, shorter during POST (PRE, mean 0.140 s, median 0.110 s; POST, mean 0.127 s, median 0.100 s,  $P < 0.001$ , rank-sum test).

Hippocampal frames tended to occur at a rate of  $44.72 \pm 3.47$  per min during

SWS ( $n = 44,479$  during 16 sleep sessions from four rats). There existed no difference in incidence rate between PRE or POST (PRE,  $40.54 \pm 4.99$  per min; POST  $48.90 \pm 4.65$  per min;  $P = 0.240$ , t-test). The duration of hippocampal frames tended to be longer during POST (PRE, mean  $0.695$  s, median  $0.370$  s; POST, mean  $0.844$  s, median  $0.44$  s,  $P < 0.001$ , rank-sum test) and also displayed a slightly more elevated firing rate per tetrode (PRE, mean  $36.10$  Hz, median  $27.19$  Hz; POST, mean  $39.01$  Hz, median  $29.47$  Hz,  $P < 0.001$ , rank-sum test). The periods of depolarization between hippocampal frames tended to be only slightly, but significantly, shorter during POST (PRE, mean  $0.164$  s, median  $0.115$  s; POST, mean  $0.156$  s, median  $0.110$  s;  $P < 0.001$ , rank-sum test). Overall, there was no difference in duration between thalamic and hippocampal frames (ADN, mean  $0.718$  s, median  $0.420$  s; CA1, mean  $0.779$  s, median  $0.405$  s,  $P = 0.782$ , rank-sum test) and only a small difference in inactivity periods between frames (ADN, mean  $0.133$  s, median  $0.105$  s, CA1, mean  $0.160$  s, median  $0.115$  s,  $P < 0.001$ , rank-sum test).

Next, we tested if activity frames across areas were related. We found a tendency for thalamic frames to start and end ahead of hippocampal frames (Figure 7E). Cross-correlograms revealed significant correlations during a range of lags for both frame onset ( $-180$  to  $80$  ms,  $P < 0.005$ , t-test) and offset ( $-140$  to  $50$  ms,  $P < 0.005$ , t-test) times. Weighted mean lags with significant correlations (correlation coefficient used as weights) indicated that, on average, thalamic frames led hippocampal frames by  $51$  ms at frame onset and by  $37$  ms during the offset phase. Our results are in close agreement with earlier findings showing cortical frames leading hippocampal frames by  $50$  ms at onset and  $40$  ms at offset times (Ji & Wilson 2007).

Given that frame activity is surrounded by periods of hyperpolarization, it is possible that the MUA cross-correlogram depicted in the left panel of Figure 7B could have resulted from the alignment of hippocampal MUA bursts with thalamic hyperpolarization periods. In this case, rather than indicating an interaction between structures, the correlogram might only reflect the transition periods of the underlying frame activity. To investigate this possibility, we recalculated the MUA cross-correlogram within periods of at least 300 ms duration in which depolarized activity in the two areas overlapped ( $n = 19,511$ ). Despite the additional selection restriction, the cross-correlogram continued to display significant correlations between thalamic and hippocampal MUAs at -90 ms ( $P = 0.008$ , t-test) and 100 ms ( $P = 0.004$ , t-test) lags (Figure 7B, right). Because inter frame hyperpolarization segments were excluded, this result further strengthens the notion that activities in the two areas can interact during frame periods and are not simply the result of alignments of thalamic hyperpolarization epochs with ongoing hippocampal MUA.

Lastly, we employed our Bayesian decoding algorithm (20 ms bin) to investigate thalamic and hippocampal ensemble activities during overlapping frame periods. Figure 8A shows six examples of the estimated position and orientation patterns displayed by place cells during periods of elevated MUA from three different rats. The top panels in each set display the corresponding estimated orientation profiles from HD cell activity before (120 ms), during and after (120 ms) hippocampal MUA bursts. Thalamic and hippocampal MUAs are depicted at the bottom of each set to highlight the time-offset relationship revealed by the earlier cross-correlation analysis. The examples shown here highlight several differences between HD and place cell activities during SWS. A common pattern

found in all these examples is that thalamic activity tended to reflect constant orientations during each of the different decoding periods. In addition, the examples on the left column reveal that place cells encoded location and orientation trajectories similar to those expressed during awake behavior and awake replay. However, the examples on the right column demonstrate that more complex patterns existed that could not be accurately described by the linear fit method used for awake replay events. Given the diversity in the spatial patterns expressed by place cells as well as the seemingly piecewise constant orientation profiles encoded by HD cells during SWS, we chose to use the variance in the orientation estimations as a measure to differentiate the spatial content of HD and place cells (Fisher 1993). We analyzed events defined by large hippocampal MUA bursts (three standard deviations above mean level of activity,  $n = 3,586$ ) occurring within common periods of depolarization. Figure 8B shows the cumulative distribution function (CDF) of the circular variance for thalamic orientation estimations in periods of 120 ms duration preceding and succeeding (red dotted lines) MUA bursts (red solid line). The CDF corresponding to hippocampal decoding is also displayed (black line). The plot illustrates the strong tendency for HD cells to encode orientations with lower variability in any one period compared to the patterns encoded by place cells ( $P < 0.001$ , Kolmogorov-Smirnov test). Interestingly, when measuring the variability in thalamic orientation estimates from the period before to the period after each hippocampal MUA burst, there was a significant increase relative to each period in isolation ( $P < 0.001$ , Kolmogorov-Smirnov test, Figure 8C) which was qualitatively similar to the variability obtained from hippocampal estimations. This result suggests that there is a slow progression in thalamic decoded

orientations, which could be the result of a bidirectional interaction between hippocampal and thalamic cells during SWS.

## **Discussion**

Several lines of evidence suggest important contributions from ADN and hippocampus during spatial memory and navigation. Here we have demonstrated, using a Bayesian decoding algorithm, that place and HD cells faithfully reflect the spatial behavior of the animals during active locomotion. Our observation is consistent with the notion that the collective activity of these cells provide the basis for a sense of location and orientation and is useful in guiding navigation. By contrast, during periods of awake immobility, two differences between thalamic and hippocampal activities became apparent. At the population level, bursting activity was prevalent in the hippocampus and nearly absent in the thalamus. At the ensemble level, the spatial content encoded by the two areas was independent of one another. In line with previous reports, we identified the replay of sequential locations during brief hippocampal MUA bursts (Foster & Wilson 2006; Csicsvari et al. 2007; Diba & Buzsáki 2007; O'Neill et al. 2008; Davidson, Kloosterman & Wilson 2009; Karlsson & Frank 2009). However, HD cells did not exhibit a similar replay of orientation trajectories. This finding reveals that, while place and HD cells are normally coupled during navigation, they can be dissociated according to behavioral or cognitive demands. It was initially suggested that awake hippocampal replay could represent a means for the consolidation of particular events associated with the represented trajectory. Recent data suggest that an

alternative or complementary function of replay could be the expression of all navigational paths available to the rat during active behavior (Gupta et al. 2010). If, in fact, rats use this information in the evaluation of routes, our finding implies that directional information is not explicitly incorporated in the assessment of potential maze paths. The independence evidenced by our observation is reminiscent of a study in which lesions of the hippocampus had little or no effect on the firing of HD cells demonstrating some degree of separation between the two systems (Golob & Taube 1997). At the same time, our result is in contrast with the strong influence HD cells have been proven to exert on hippocampal firing. For instance, manipulations that abolish the tuning of HD cells, including lesions to thalamic or subicular HD cells, have detrimental effects on the stability and coherence of hippocampal firing fields (Taube, Kesslak & Cotman 1992; Stackman, Clark & Taube 2002; Calton et al. 2003). Note, however, that lack of thalamic replay does not entirely rule out the potential contribution of HD signals to hippocampal replay. It is possible that the sustained directional input provided by HD cells could influence features of replay. For example, HD cell activity could bias the starting location of the replayed trajectory towards positions associated with the rat's current orientation. We were unable to directly test this hypothesis in our study because, in most of the detected events, the initial replayed position tended to coincide with the current location of the animal. Further experiments involving the manipulation of HD cell activity will be useful in establishing their participation in awake hippocampal replay.

Assuming that HD cells passively influence replay, it is conceivable that thalamic burst firing during subsequent SWS could also serve as a physiological

cue to bias the spatial content of hippocampal activity. The hypothesized thalamic influence could benefit from or be manifested as periods in which the activities in the two brain structures are related. Consistent with this proposal, we show that population activities in ADN and hippocampus are correlated during SWS. Specifically, we found that hippocampal MUA bursts were, on average, flanked by bursts of thalamic activity. The fact that periods of elevated thalamic firing occur before and after hippocampal bursts with similar probability is suggestive of bidirectional communication between these areas. The wide range in delays between bursts across structures are well within physiological ranges reported during sleep and awake states (Siapas, Lubenov & Wilson 2005; Wierzynski et al. 2009), and might be indicative of multi synaptic connections between the hippocampus and ADN,

It has been demonstrated, using intracellular recordings, that thalamic activity is organized in alternating periods of collective depolarization (up-states) and brief hyperpolarization epochs (down-states) during SWS (Steriade et al. 1993). Similarly, hippocampal activity was recently shown to display an analogous activity organization principle (Wolansky et al. 2006; Ji & Wilson 2007). Here we demonstrated, using extracellular recordings, that both areas oscillate between periods of elevated firing and periods of no activity. Importantly, we found that the depolarized states across areas were correlated. On average, thalamic up-states led hippocampal depolarized states. The relevance of this correlation relates to the hypothesized function attributed to up-states as a functional unit for sleep-related processes involving multiple brain structures. Previous work identified a similar correlation between depolarized states in the visual cortex and hippocampus (Ji & Wilson 2007). In that study, hippocampal depolarization

was hypothesized to be the result of cortical drive given a 50 ms lead time in cortical activity. Our results show a remarkable similarity in the timing relationship with hippocampal frames. Note that the correlations are not limited to the boundaries of the depolarized states. Hippocampal and thalamic MUAs continue to be significantly correlated within depolarized states and the shape of the correlation function strongly suggests an ongoing bidirectional interaction between structures. Interestingly, the spatial content in periods surrounding and including large hippocampal MUA bursts demonstrated a tendency for HD cells to encode orientations with little time variation in each epoch. By contrast, hippocampal cells tended to exhibit larger orientation variability suggestive of expression of location trajectories. These variability patterns display some resemblance to the spatial content encoded by HD and place cells during awake replay in which HD cells reflect the animal's current (and constant) orientation. Because the variance in orientation increases when considering all three periods as a continuous segment, it is possible that HD cells exhibit orientation progressions during SWS. Such progression could be the result of hippocampal influence on thalamic activity and could be a useful mechanism for communication with cortical areas associated with the thalamus. In this regard, it is important to point out that corticothalamic interactions have been linked to the generation of the major rhythmic activities that characterize SWS. Specifically, thalamic cells generate spindle (7 - 14 Hz) and delta (0.5 - 4 Hz) rhythms which are grouped by the cortically-generated slow oscillation. Current knowledge about cortical and thalamic electrophysiology suggests that the onset of the cortical up-state stimulates the generation of thalamic spindles which then are fed back onto cortical circuits (Steriade et al. 1993; Steriade,

Nuñez & Amzica 1993). Coupled with our results, it is possible to suggest that the thalamus could serve as a channel to coordinate cortico-hippocampal communications. In particular, consider two previous findings regarding cortico-hippocampal interactions. An early study reported that cortical spindles and hippocampal ripples are correlated (Siapas & Wilson 1998). This relationship was postulated to reflect the transfer of mnemonic information from hippocampal to cortical circuits. A key assumption about the presumed transfer of such information is that cells involved in spindles and ripples were previously co-active and represented complementary aspects of the same awake behavior. More recently, neurons from the visual cortex were shown to replay activity patterns along with hippocampal patterns during sleep up-states (Ji & Wilson 2007). Replayed patterns in both areas were previously co-expressed during periods of active behavior. The known directional flow of information between thalamus and cortex, as well as the present MUA correlations between ADN and CA1 raise the possibility that thalamic activity could bias the selection of hippocampal and cortical units that participate in sleep replay by exciting cortical and hippocampal cells with which they had previous associations during active behavior. Alternatively, they could aid in the presumed cortical drive of hippocampal activity (Hahn, Sakmann & Mehta 2006; Hahn, Sakmann & Mehta 2007; Mehta 2007). Additional work involving the simultaneous recording of cortical, thalamic and hippocampal areas would be useful in testing this proposal.

## Methods

### *Rats and experimental procedures*

Four male Long-Evans rats (500 – 600 g) were implanted with arrays of 18 independently movable tetrodes aimed at the anterior dorsal thalamus (ADN; -2.1 mm AP, 1.3 mm ML, relative to bregma) and the CA1 layer of the dorsal hippocampus (CA1; -3.6 mm AP, 2.1 mm ML, relative to bregma). A bipolar electrode was inserted in the neck muscle to record the electromyogram (EMG). Surgical procedures and behavioral testing were approved by the Committee of Animal Care at Massachusetts Institute of Technology and followed US National Institute of Health guidelines.

After implantation, tetrodes were advanced over the course of several days until they rested near the target areas. After the initial positioning, the depth of individual tetrodes was adjusted to increase unit yield. To maximize signal stability, recordings took place at least 12 hours following the last depth adjustment. Spikes crossing a preset threshold on any of the four leads of a tetrode were recorded at 32 kHz for subsequent analysis. A custom written software (Xclust, M.A.W) was used to identify and isolate individual cells based on spike amplitude and waveform. Multi unit activity (MUA) was defined as the set of spikes with a minimum amplitude of 70  $\mu$ V on any of the four wires of a tetrode. Local field potential (LFP) and EMG signals were bandpass filtered between 1 – 475 Hz and sampled at 2 kHz. Position and head direction were measured by the centroid and relative angle between a pair of diode arrays, respectively. The diode arrays were mounted on the head-stage and aligned with the long axis of the rat. Sampling took place uninterruptedly at 30 Hz by an

overhead camera.

During the initial tetrode positioning period, rats were exposed to an elevated circular track in a secondary room to encourage exploratory activity. Rats were rewarded for spontaneous alternations between clockwise and counterclockwise trajectories. Data acquisition took place in a different room and on a novel maze about a week after the last exposure to the training track. In the new task, rats ran back and forth between two points on either side of a high wall divider attached to an elevated circular maze (125 cm diameter, 10 cm width; Figure 3A). Food reward was given when the rat successfully traversed the entire track to reach the food well. No behavioral criterion for task performance was required. A typical experimental session involved 1 - 3 hr sleep epochs before (PRE) and after (POST) a 25 - 35 min period of active exploration (RUN). Both sleep sessions were conducted on an elevated dish within a high walled enclosure away from the maze. The sessions reported here correspond to days in which at least 5 head direction cells were recorded and are not necessarily matched for each rat's familiarity with, or running performance on, the track.

### *Receptive fields*

One dimensional place tuning was measured on linearized coordinates. Linearization took place by transforming each point's Cartesian coordinate (x,y) to its corresponding polar coordinate ( $\rho, \theta$ ), where  $\theta$  was measured relative to the line joining the circle center and the starting position on the track. The angle coordinate was then transformed into distance units by determining the length of the arc it described on a circle with radius 62.2 cm.

Position (head direction) tuning was quantified by counting the number of spikes

fired in non overlapping 10 cm (10 deg) bins and dividing them by the total amount of time the rat occupied (faced in the direction specified by) each bin. Only spikes fired when the rat had a linear speed > 15 cm/s were used for calculation of hippocampal receptive fields. All spikes, irrespective of linear or angular velocity, were used to assess the directional tuning of thalamic cells.

### *Firing characteristics*

Bursting index was defined for each cell as the percentage of spikes within a burst divided by the total number of spikes fired by the cell. A burst consisted of sets of spikes separated by 5 ms or shorter inter spike intervals (ISI) and whose first spike was preceded by an ISI longer than 100 ms (Ramcharan, Gnadt & Sherman 2005).

Theta modulation was assessed by means of the cell's autocorrelation function. Spike trains were converted into firing rates with 10 ms resolution. The autocorrelation coefficient at lag  $\Delta t$  was calculated with equation (1), by making f and g both represent the same cell's firing rate.

$$Xcor(\Delta t)_{fg} = \frac{\sum_{t=1}^n (f(t) - \bar{f})(g(t+\Delta t) - \bar{g})}{\sqrt{\left(\sum_{t=1}^n (f(t) - \bar{f})\right)^2} \sqrt{\left(\sum_{t=1}^n (g(t) - \bar{g})\right)^2}} \quad (1)$$

where

$$\bar{f} = \frac{1}{n} \sum_{t=1}^n (f(t)) , \quad \bar{g} = \frac{1}{n} \sum_{t=1}^n (g(t)) \quad (2)$$

Peaks in the autocorrelation function were identified and the inverse of the mean distance between them was taken as the preferred frequency at which cells were modulated. Differences in firing mode or theta modulation between different behavioral states were statistically assessed by means of the rank-sum test.

### *Position/Head direction estimation*

We used a Bayesian decoding algorithm to estimate position (head direction) in non overlapping time bins based on the activity of cell ensembles (Zhang et al. 1998; Johnson, Seeland & Redish 2005; Davidson, Kloosterman & Wilson 2009). Decoding requires we know two things about each cell: its receptive field and the number of spikes it fires in the estimation window. Estimation returns the likelihood with which each position (head direction) could result in the observed ensemble firing profile and is given by:

$$P(\mathbf{x}|\mathbf{n})=C(\tau,\mathbf{n})P(\mathbf{x})\left(\prod_{i=1}^N f_i(\mathbf{x})^{n_i}\right)\exp\left(-\tau\sum_{i=1}^N f_i(\mathbf{x})\right) \quad (3)$$

where  $C(\tau,\mathbf{n})$  is a normalization factor,  $P(\mathbf{x})$  represents the position (head direction) prior probability,  $f_i(\mathbf{x})$  is the receptive field of the  $i$ th recorded cell and  $n_i$  are the number of spikes fired by the  $i$ th cell in the observation window  $\tau$ . Prior probabilities for position and head direction were assumed to be uniform. Use of bold notation for  $\mathbf{x}$  and  $\mathbf{n}$  stresses the fact that estimation likelihood is expressed for the range of all possible values the spatial variable can take and that its calculation takes into account the simultaneous activity of

all recorded cells. Decoding errors were quantified by choosing the estimation with maximum likelihood and comparing it to the actual value of the spatial variable during the estimation time bin. Differences in estimation errors during different behavioral epochs were tested statistically by means of the rank-sum test.

#### *Position replay detection during awake immobility*

Epochs of immobility during RUN were defined as having linear speeds lower than 5 cm/s. Within those times, periods of elevated hippocampal MUA were identified. Events whose peak amplitude exceeded the mean level of activity during immobility by three standard deviations and which contained spikes from at least four different hippocampal cells were considered for analysis. A minimum duration of 80 ms was required. Duration was measured as the period in which hippocampal MUA was above its mean value. Events that satisfied the above criteria became the pool of candidate events.

Replay episodes were defined as series of estimated positions, within candidate events, that described complete or partial track traversals at a constant speed. Replay detection has been described with greater detail elsewhere (Davidson, Kloosterman & Wilson 2009). Briefly, a line-finding algorithm (Toft 1996) was used to score all the trajectories that could possibly be described by the estimated positions. The score consisted of the mean likelihood calculated from the individual position constituents of each trajectory. The trajectory with maximum score was selected. The statistical significance of the resulting replay was assessed by comparing the distribution of scores resulting from three

different randomization procedures of the original data as follows: random reassignment between spike trains and place cells prior to position estimation, random circular shifts of position estimates of each estimation window and random selection of estimation bins from the entire pool of candidate events arranged to form pseudo events that matched the duration of the replay event under analysis. Replays with Monte Carlo p-values  $< 0.05$  were included in the analysis.

### *Sleep classification*

Four different vigilance states were identified during the periods rats spent in the sleep box enclosure, namely: awake, slow wave sleep (SWS), rapid eye movement sleep (REM) and intermediate sleep. Classification was based on the presence of lfp rhythms that characterize each state (Robert, Guilpin & Limoge 1999). Mean power in different frequency bands was calculated with a 2 s sliding window (1s step). Power in the delta (0.5 - 4 Hz) and theta (5 - 12 Hz) bands were quantified from thalamic lfp. Power in the ripple (100 - 300 Hz) band was measured from hippocampal lfp. Periods of elevated activity in the neck EMG were classified as awake irrespective of lfp activity. SWS was identified as periods, of at least 30 s duration, in which power in both the delta and ripple bands were above their corresponding mean level of activity. SWS episodes separated by brief (less than 2 s) decreases in delta and ripple activities were bridged into single events. REM was identified as epochs with high theta power relative to power in the delta band. Specifically, epochs in which the theta/delta ratio was above its mean level by one standard deviation. Periods that failed to

be identified as awake, SWS or REM were classified as intermediate sleep.

### *Population activity cross-correlation during SWS*

The population activity organization within hippocampus and thalamus, as well as their interactions was assessed through MUA. First, MUA was converted into spike count vectors with 5 ms resolution. The resulting spike count series were smoothed with a Gaussian kernel ( $\sigma = 10$  ms). To assess the degree of interaction between areas, hippocampal and thalamic spike count vectors were cross-correlated according to equation (1). Hippocampal series were used as the reference signals ( $f$  in equation 1). We used a t-test to evaluate the significance of the peak correlations against the null hypothesis that thalamic and hippocampal MUAs were uncorrelated with a correlation coefficient of zero. At each time lag, statistical testing incorporated data from 18 sleep sessions.

### *Up state definition and cross-correlation*

Frames of activity were defined from the aggregate binned and Gaussian smoothed MUA (5 ms bin,  $\sigma = 10$  ms) within each structure separately. A frame was defined as a period in which MUA spike counts were consistently above a preset activity threshold (0.110 spike count for ADN and 0.330 spike count for CA1). Periods that exceeded the activity threshold but were separated by a brief activity gap (50 ms for ADN, 60 ms for CA1) were consolidated into a single activity period.

The start and end times of activity frames were independently converted to

event rates by binning sleep episodes with a sliding non-overlapping 10 ms window. Cross-correlation coefficients were calculated according to equation (1) and significance evaluated with the use of a t-test as described above. Lags exhibiting significant correlations ( $P < 0.005$ ) were identified and their correlation values were used as weights to determine the average time lead-lag relationship between hippocampal and thalamic frame onset and offset times.

#### *MUA and spatial decoding during overlapping frame activity*

Periods of overlapping depolarized frames were identified. We recalculated the cross-correlation between hippocampal and thalamic MUAs as described above considering only coincident frame periods lasting at least 300 ms.

We decoded orientation and position patterns from HD and place cells using 20 ms bins within epochs defined by hippocampal MUA bursts exceeding the mean level of SWS activity by three standard deviations. We distinguished three different periods: epochs of large hippocampal MUA activity and 120 ms duration periods around them. We assessed the circular variance (Fisher 1993) on the orientation estimates from each structure within each period, or during the longer interval resulting from their concatenation. The statistical difference between the distribution of variances was assessed using the Kolmogorov-Smirnov test.



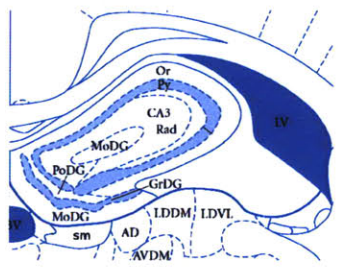
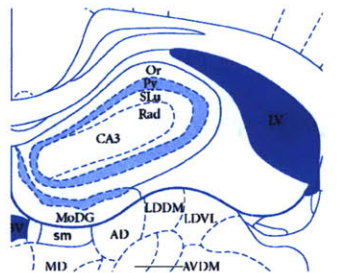
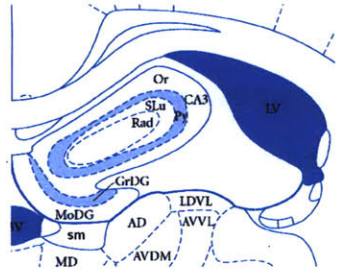
## **Figure 1. Localization of thalamic recording sites**

(A) Schematic diagrams of three coronal slices showing the location of the anterior thalamic nuclei. Slices (from top to bottom) correspond to coronal sections at 1.950, 2.075 and 2.200 mm posterior to bregma. Note that, in each slice, the dorsal division of the anterior thalamus (AD) is located below the dentate gyrus and immediately adjacent to the stria medularis (sm).

(B) Photographs of five coronal slices spanning 200  $\mu\text{m}$  around the recording cannula. Distance between consecutive slices is 50  $\mu\text{m}$ . Partial tetrode tracks are visible on all slices as dark vertical lines. Electrolytic lesions (white arrows) confirm the location of the tetrode tips in the area corresponding to the anterior thalamus.

Abbreviations: AD, anterior dorsal thalamic nucleus; AVDM, anterior ventral dorsal medial thalamic nucleus; AVVL, anterior ventral thalamic nucleus ventrolateral part; CA3, CA3 hippocampus; GrDG, granular layer of dentate gyrus; LDVL, lateral dorsal thalamic nucleus ventrolateral part; LV, lateral ventricle; MD, medial dorsal thalamic nucleus.; MoDG, molecular layer of the dentate gyrus; Or, stratum oriens; PoDG, polymorph layer of the dentate gyrus; Py, stratum pyramidale, Rad, stratum radiatum; SLu, stratum lucidum; sm, stria medularis; 3V, dorsal third ventricle.

A



B

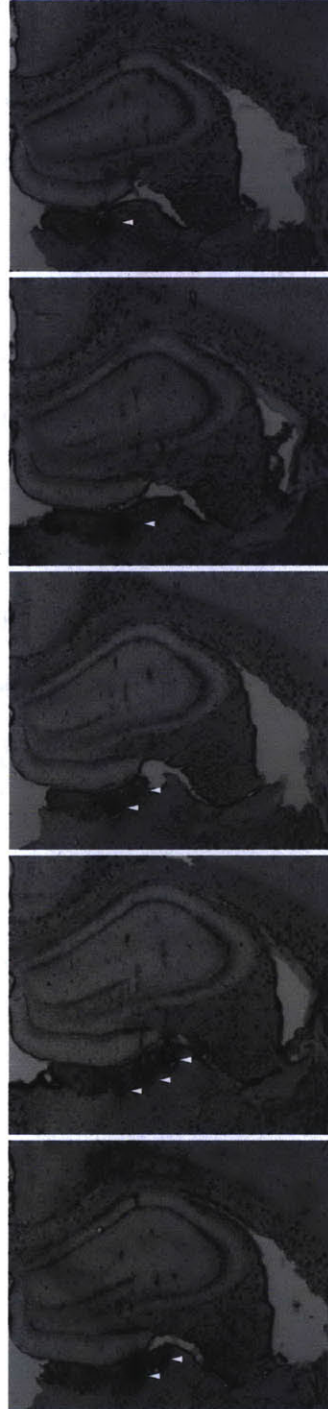


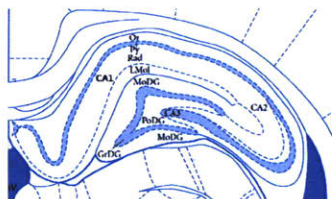
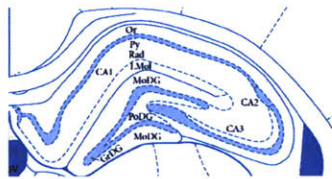
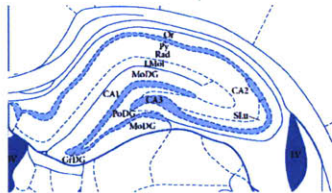
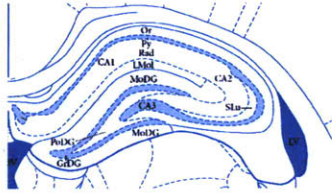
## **Figure 2. Localization of hippocampal recording sites**

(A) Schematic diagrams of four coronal slices showing the different subregions of the hippocampus. Slices (from top to bottom) correspond to coronal sections at 3.25, 3.50, 3.75 and 4.00 mm posterior to bregma.

(B) Photographs of four coronal slices corresponding to the diagrams in (A). Electrolytic lesions (white arrows) confirm the location of the tetrode tips in the area corresponding to the CA1 layer of the hippocampus.

Abbreviations: CA1, CA1 hippocampus; CA2, CA2 hippocampus; CA3, CA3 hippocampus; GrDG, granular layer of dentate gyrus; LMol, stratum lacunosum moleculare; LV, lateral ventricle; MoDG, molecular layer of the dentate gyrus; Or, stratum oriens; PoDG, polymorph layer of the dentate gyrus; Py, stratum pyramidale, Rad, stratum radiatum; SLu, stratum lucidum; sm, 3V, dorsal third ventricle.

A



B

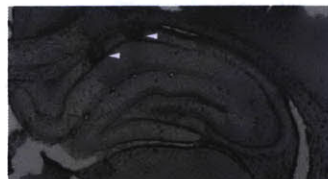
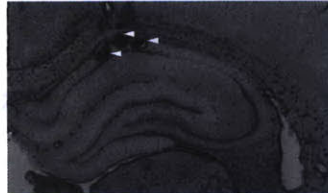


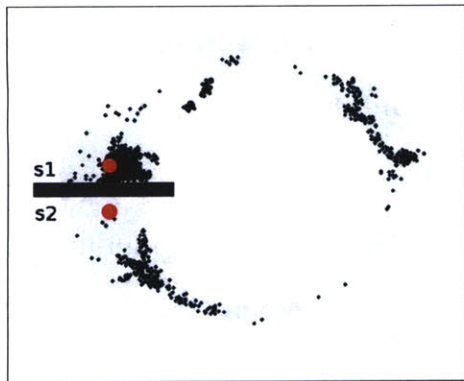
### **Figure 3. Behavioral task and receptive fields**

(A - B) Data from one rat showing cumulative records of visited positions (gray) during 33 minutes of RUN behavior on a circular track. Rats ran back and forth between the end points of the track (s1, s2, red circles) for food reward. Dark-gray rectangle represents high wall divider. Black dots correspond to spikes fired by a thalamic HD cell (A) and a hippocampal place cell (B). Note that, in this case, place cell firing is restricted to only two locations on the track. By contrast, firing of HD cell is not location-specific.

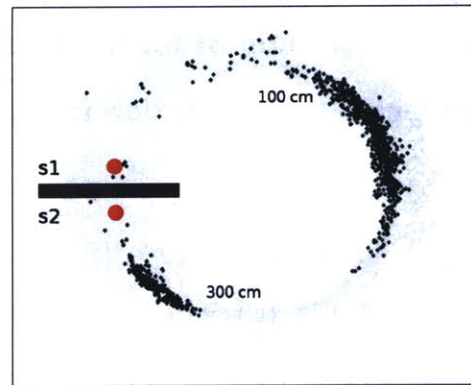
(C) Normalized receptive fields of seven HD cells. Receptive fields were calculated during RUN with a 10° bin size.

(D) Normalized receptive fields of 35 place cells. Receptive fields were calculated at 10 cm resolution. Note that receptive fields are expressed as linear distance from the food well labeled s1 in (A) and (B).

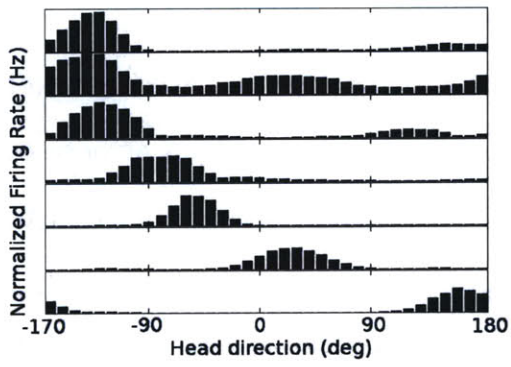
A



B



C



D

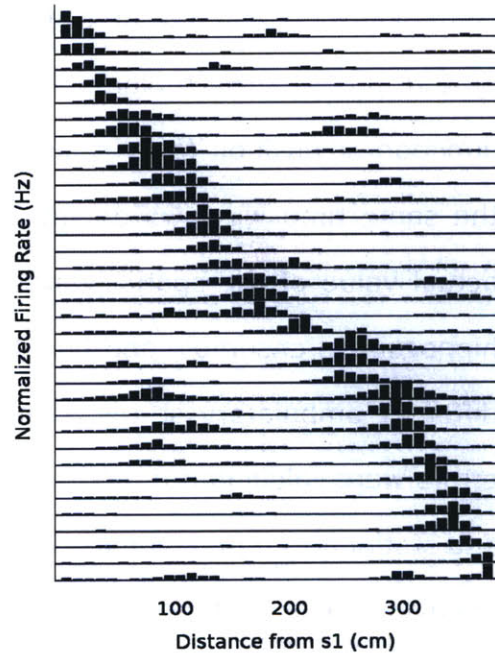
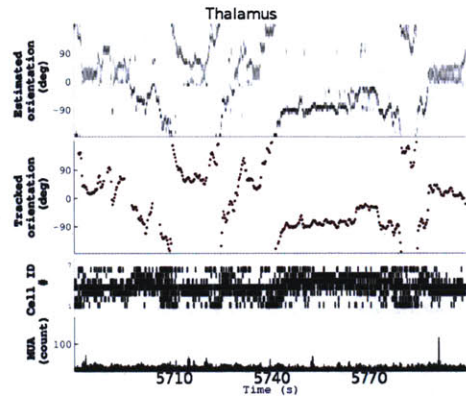


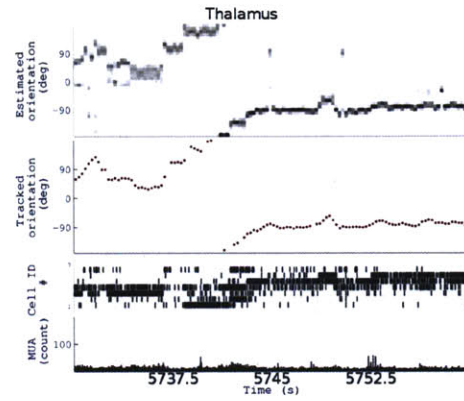
**Figure 4. Hippocampal cell ensembles faithfully reflect spatial behavior during periods of locomotion only; thalamic cell ensembles accurately reflect rat's orientation irrespective of ambulatory state.**

(A,C) Top panels display estimated head orientation (gray scale) during a 120 s (A) or 30 s (C) window during maze exploration. Actual head direction is represented by red dots in second panel. Estimation was based on spiking activity of seven thalamic HD cells depicted in third panels. Each row corresponds to a different cell and each tick represents an action potential. Bottom panels show thalamic MUA. (B,D) Top two panels show estimated head direction or position (gray scale) based on hippocampal spiking activity during the same time windows depicted in (A) and (C). Red dots correspond to the actual value of the spatial variable being displayed. Bottom two panels show hippocampal ensemble and population activities. (E-G) Estimation errors during different ambulatory states. Head direction (E,F) and position (G) estimation errors were calculated during movement (left columns, linear speed > 15 cm/s) and stationary (right columns, linear speed < 6 cm/s) periods during exploratory behavior. Error distributions correspond to aggregate data across rats. Red, dotted lines correspond to median error values.

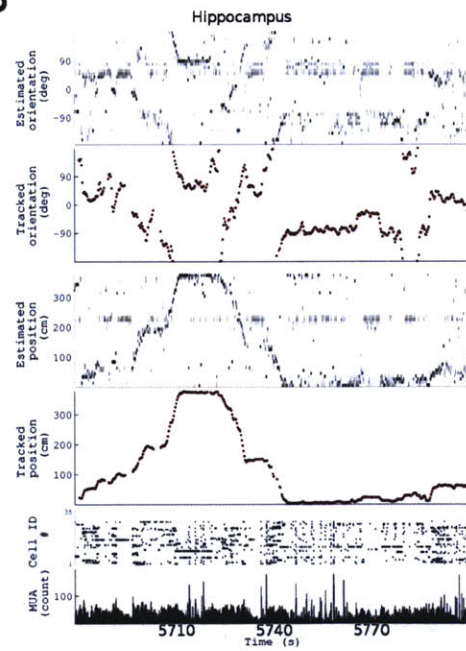
A



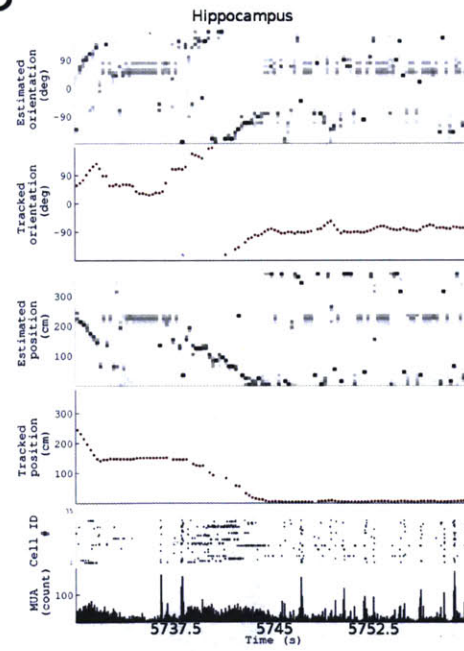
C



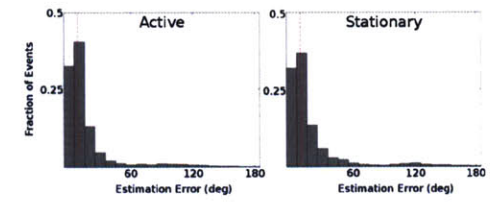
B



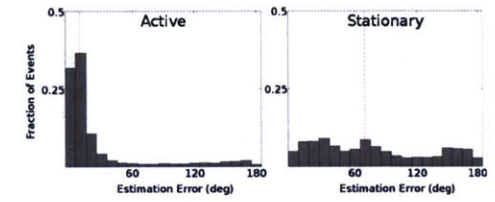
D



E



F



G

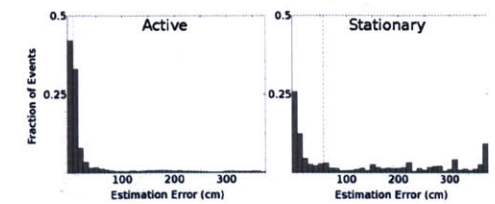
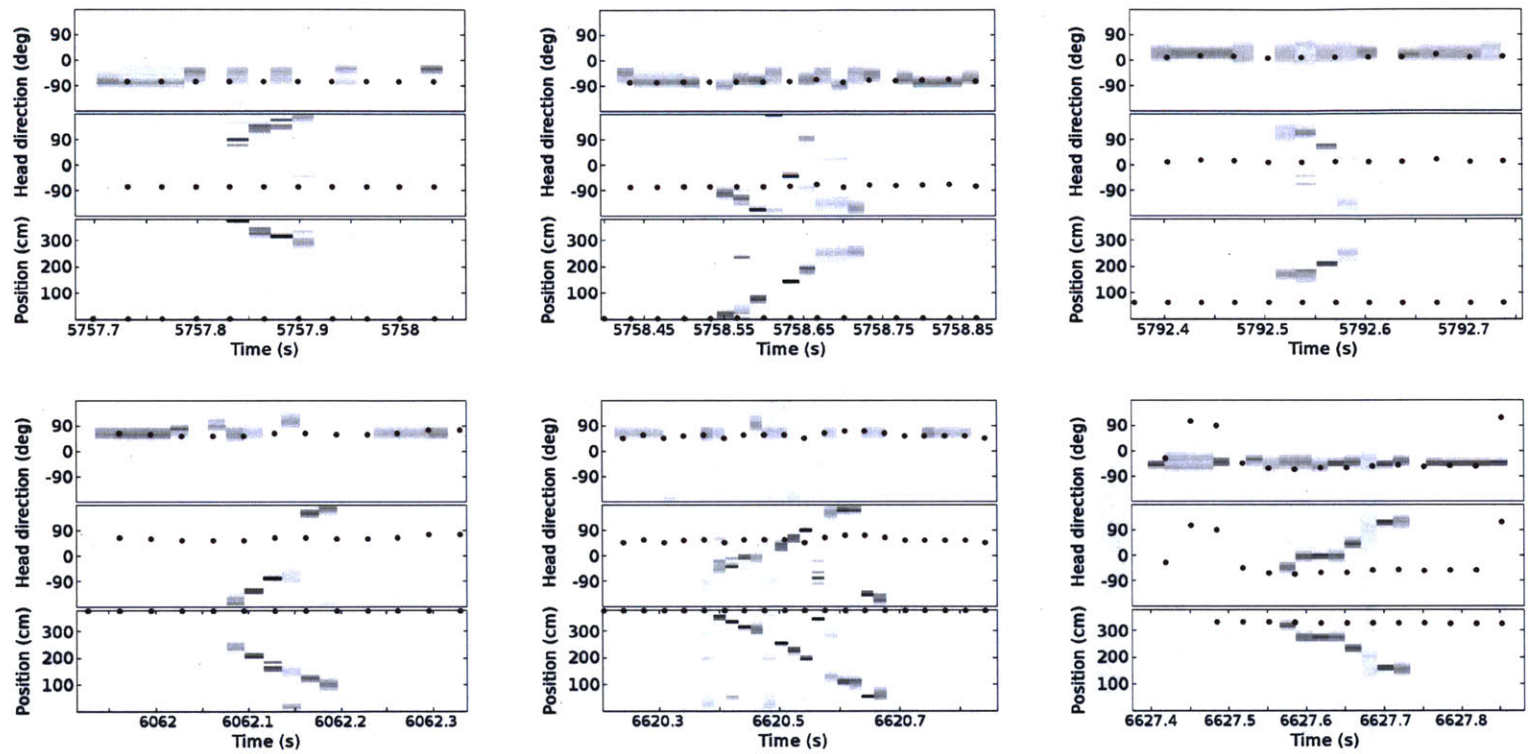


**Figure 5. Hippocampal and thalamic spatial representations are decoupled during periods of immobility.**

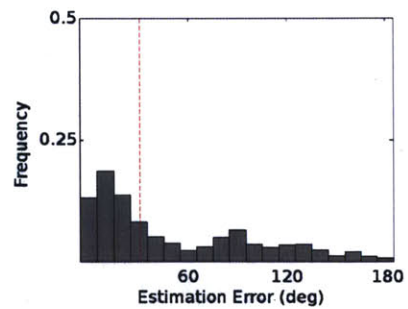
(A) Thalamic and hippocampal based estimation of head direction or position during periods of immobility. For each set, top and middle panels display estimated head direction (gray scale) based on thalamic (top) or hippocampal (middle) spiking activity. Tracked head direction is indicated by red dots. Bottom panels show estimated position (gray scale) based on hippocampal activity. Actual position is indicated by red dots. Top row corresponds to data from rat in Figure 4. Bottom row corresponds to examples from two additional rats. Thalamic-based estimations are shown for an extended 120 ms before and after hippocampal events.

(B - D) Distributions of estimation errors during immobility periods. Errors were calculated for estimated head direction based on (B) thalamic or (C) hippocampal activities. Position estimation errors (D) were based on hippocampal activity. Estimation errors were calculated during time windows defined by significant position replay events ( $N = 319$ ) and correspond to data pooled across three rats. Red dotted lines correspond to median errors.

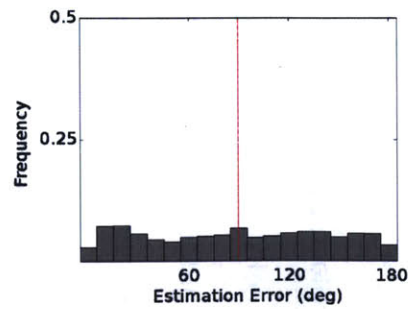
A



B



C



D

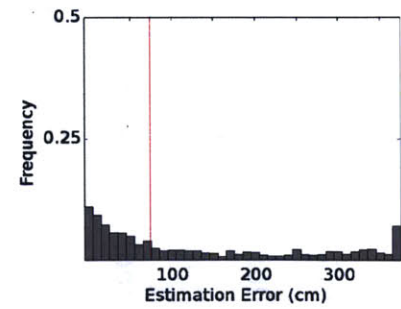


**Figure 6. Firing mode during different behavioral states.**

(A-C) Two dimensional ISI and autocorrelation plots for a typical thalamic HD cell during (A) RUN, (B) SWS and (C) REM. The presence of a single cluster on the 2-D ISI plot indicates that HD cells fire in a predominantly tonic mode during RUN and REM. By contrast, during SWS, four spike clusters are clearly identified consistent with a predominantly burst firing mode. Lack of side peaks in autocorrelograms indicate no rhythmic firing of thalamic cells.

(D-F) Two dimensional ISI and autocorrelation plots for a typical hippocampal place cell during (A) RUN, (B) SWS and (C) REM. Contrasting with HD cells, place cells exhibited bursting activity in all behavioral states. Side peaks in the autocorrelation functions demonstrate rhythmic firing in the theta range during RUN and REM, but not SWS.

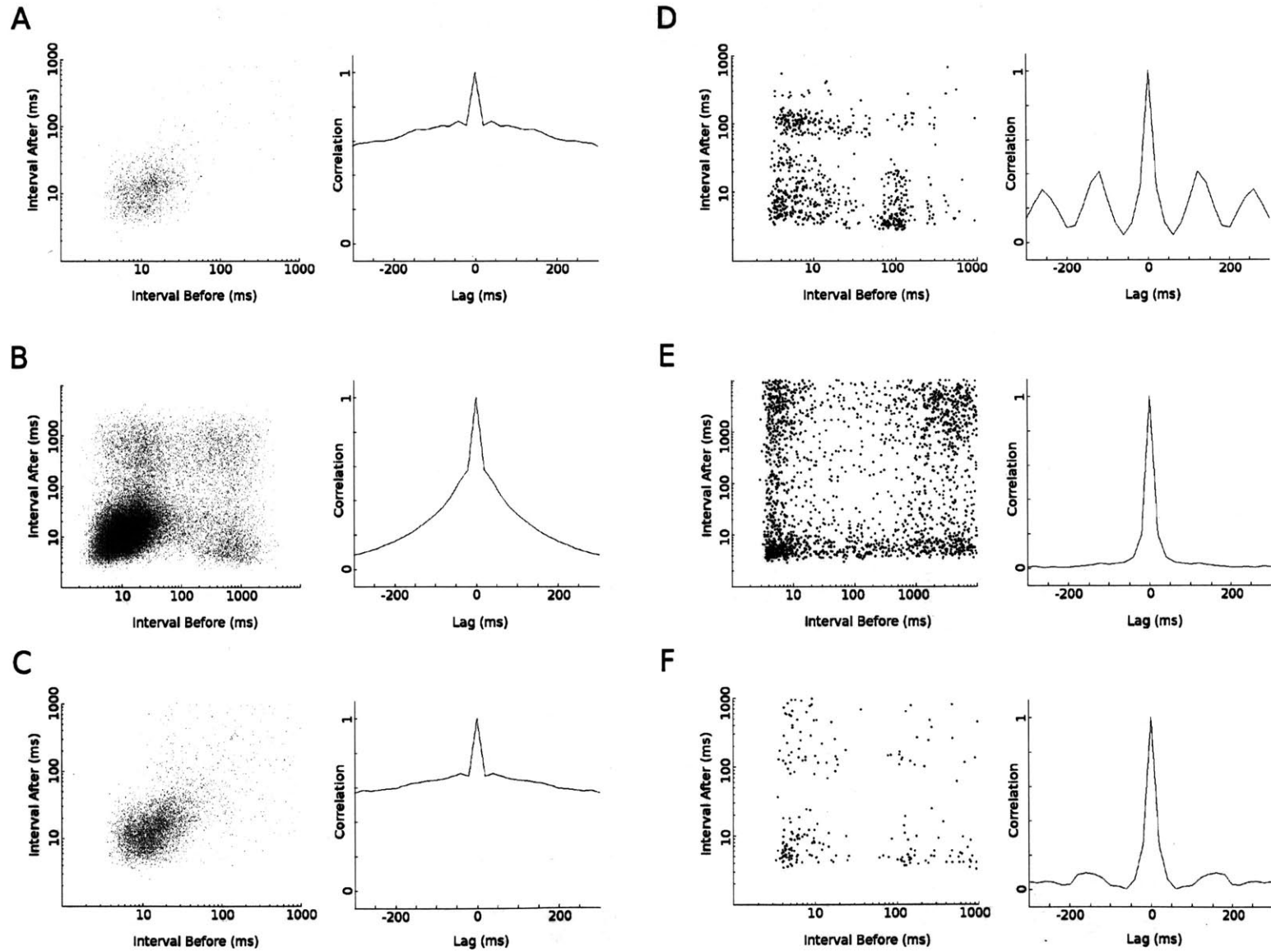


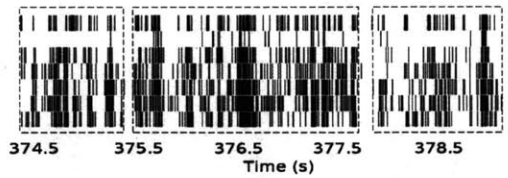
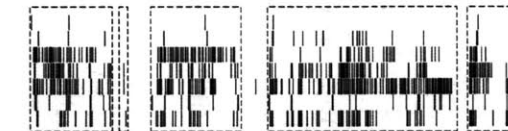
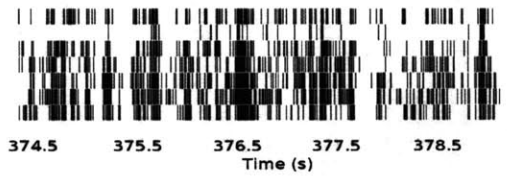
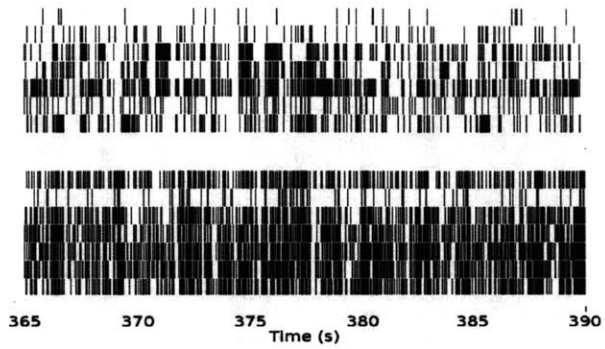
**Figure 7. Population activity coordination during slow wave sleep.**

(A) Thalamic and hippocampal MUA during SWS. Top panel depicts MUA activity during a 25 s sleep period. Each tick mark represents a spike and each row corresponds to a different tetrode. Spikes do not necessarily represent isolated cells. Top row set corresponds to thalamic tetrodes. Bottom row set corresponds to hippocampal tetrodes. Middle and bottom panels correspond to a 5 s activity window illustrating the alternation in up and down states in population activity in the two areas. Dash outlines in bottom panel highlight elevated activity frames detected with the parameters used in the study.

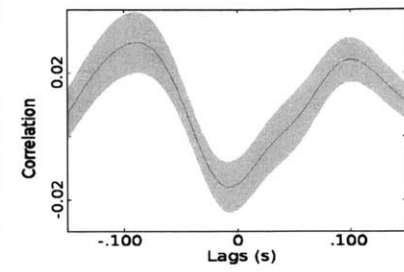
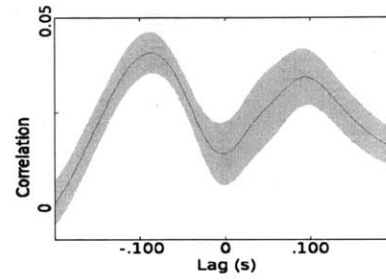
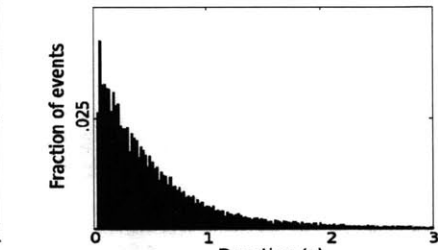
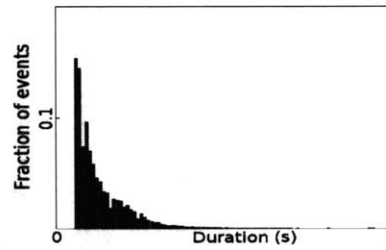
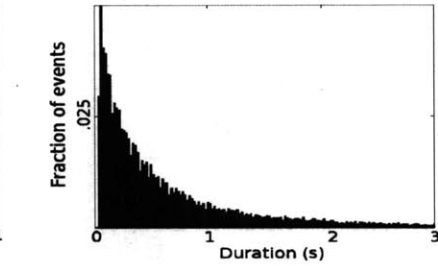
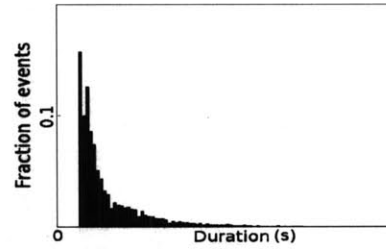
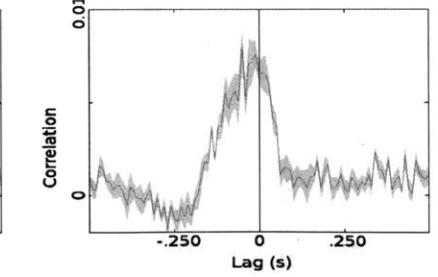
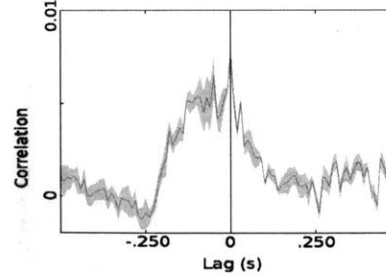
(B) Average cross-correlogram between thalamic and hippocampal MUA during SWS (left) or within overlapping depolarized states (right). Gray shade indicates s.e.m,  $n = 18$  sleep sessions. Thalamic MUA served as the reference signal in this calculation. The off-center peaks are consistent with the observation that thalamic bursts tended to occur before and after, but not during, hippocampal bursts.

(C-D) Distribution of durations of down states (left) and up states (right) for hippocampal (C) and thalamic (D) MUA.

(E) Average cross-correlogram (mean s.e.m,  $n = 18$  sleep sessions) between the start (left) and end (right) times of hippocampal and thalamic up states. Hippocampal data served as the reference signals. Peaks at negative lags indicate thalamic up states led hippocampal up states.

**A**

71

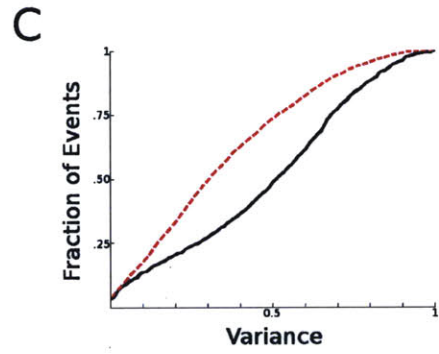
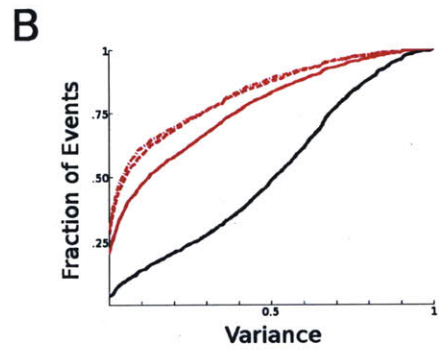
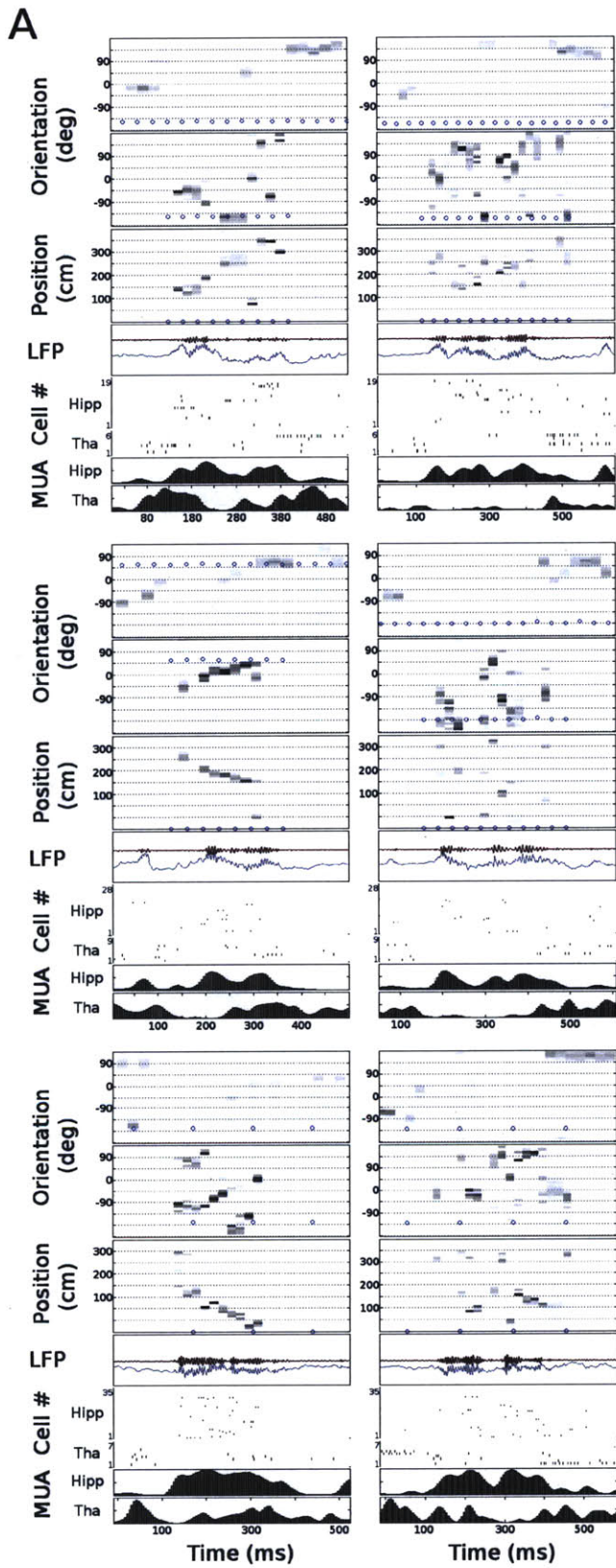
**B****C****D****E**

**Figure 8. Variance in orientation patterns encoded by thalamic and hippocampal cells suggests each structure encodes spatial trajectories at different rates during SWS.**

(A) Six examples of the spatial patterns encoded by HD and place cells during overlapping frame activity periods. Each row corresponds to data from a different rat. Each set of six panels represents the following: Top three panels correspond to the estimated orientation or position patterns decode from the spiking activities of HD (top) or place (middle and bottom) cells. Tracked orientation and position are represented by open blue circles. Middle panel displays the raw (gray) and filtered (brown) hippocampal LFP signal to highlight ripple activity. Bottom panels correspond to the spiking activities of isolated HD and place cells, along with the corresponding MUAs.

(B) Cumulative distributions of circular variance for orientation profiles during different decoding periods. Red dotted lines correspond to the variance obtained from thalamic decoding in 120 ms epochs before and after hippocampal MUA bursts. Variance during MUA bursts was measured for thalamic (red solid line) and hippocampal (black solid line) orientation patterns. Variance was significantly greater for patterns encoded by place cells than those encoded by HD cells in any one period ( $P < 0.001$ , Kolmogorov-Smirnov test).

(C) Same as (B), but here orientation variance from thalamic activity is measured in the intervals starting and ending 120 ms from hippocampal MUA bursts. Note the greater variability in the thalamic orientation patterns.





## **Chapter 3**

# **Spatial Representations in the Rat Anterior Thalamus and Hippocampus during Rapid Eye Movement Sleep**

## **Introduction**

The thalamus gates the flow of sensory information from peripheral organs and brainstem nuclei to cortical areas. This notion is supported by two observations in all mammals studied to date (McCarley, Benoit & Barrionuevo 1983; Marks & Roffwarg 1993; Burikov & Yul 1999; Ramcharan, Gnadt & Sherman 2000; Anderson et al. 2005). First, thalamic cells projecting to cortex readily respond to sensory stimuli during awake behavior. Second, during slow-wave sleep (SWS), cell firing bears little or no association to external stimuli. The difference in stimulus-response relationship is accounted for by the firing modes that thalamic cells display as a function of behavioral state. During wake cells respond in a tonic mode, firing series of conventional action potentials upon sufficient depolarization. By contrast, during SWS, cells fire periodic bursts of 2-10 action potentials independent of external drive after prolonged periods of hyperpolarization. Because the onset of sleep is characterized by such thalamic oscillatory activity, it has been concluded that the primary function of the thalamus during sleep is to isolate cortex from sensory stimuli. Importantly, during rapid-eye-movement sleep (REM), thalamic cells regain the tonic firing capacity normally associated with faithful sensory transmission during wake (Paré et al. 1990; Steriade 1992). How this change in response mode is reflected at the thalamic ensemble activity level during REM is unknown. It is possible that by virtue of being close to their firing threshold, cells generate action potentials in a random, uncorrelated, fashion. Alternatively, cell ensembles could become active in a structured way that is coherent with ongoing processes in brain areas with thalamic associations.

The hippocampus is a brain region with extensive functional connections with the thalamus. In particular, the anterior thalamic complex and hippocampus have been shown to be elements of an extended network of brain areas that support complex cognitive functions such as episodic memory and spatial navigation (Papez 1937; McNaughton et al. 2006; Aggleton 2008; Calton & Taube 2009). In the rat, subsets of cells from these structures display activities that are strongly correlated with the spatial behavior of the animal. Specifically, cells in the dorsal nucleus of the anterior thalamus (ADN) discharge as a function of the animal's head orientation relative to the environment (Taube 1995). These neurons, called head direction (HD) cells, fire in narrow regions of orientation space, irrespective of the animal's location (Figure 1). Similarly, within a given environment, pyramidal cells in the hippocampus fire when the rat occupies discrete locations in space and show little or no activity elsewhere (O'Keefe & Dostrovsky 1971). These neurons are called place cells. Under certain circumstances, the activity of place cells reflects the animal's heading direction in addition to its position (McNaughton, Barnes & O'Keefe 1983; Markus et al. 1995; Battaglia, Sutherland & McNaughton 2004). This supplementary tuning is hypothesized to arise from the direct influence of concurrent HD cell activity.

Owing to its relevance in episodic memory, hippocampal activity has been extensively studied during different behavioral states including sleep. It has been demonstrated that, during REM episodes, ensembles of place cells re-express temporally structured firing profiles that reflect familiar experiences

(Louie & Wilson 2001). Importantly, hippocampal replay takes place in the absence of explicit extra hippocampal sensory drives present during active exploration. Here we investigate whether, during REM, thalamic ensemble activity can be temporally patterned to recreate sensory information previously co-expressed with hippocampal activity during awake behavior. To address this possibility we monitor ensembles of thalamic HD cells during maze running and sleep. Besides the clear association between HD and place cells during navigation, we chose to investigate the activity of HD cells because they are primarily driven by vestibular activity (Brown, Yates & Taube 2002; Yoder & Taube 2009). Postural immobility during sleep effectively eliminates vestibular input, granting a clear distinction between thalamic activity that is intrinsically generated or externally driven.

We examined the activity of ensembles of HD cells in four rats during maze running (RUN) and sleep. We employed a Bayesian decoding algorithm to estimate orientation profiles through time, based on the firing of HD cells (Zhang et al. 1998; Johnson, Seeland & Redish 2005). The decoded head directions successfully matched the spatial behavior of the rat during RUN, which consisted of alternations between epochs of continuous time varying orientations and periods of constant head direction. Concurrently, activity in the hippocampus oscillated between periods of elevated and reduced population activity. Estimated orientation profiles and hippocampal activity were correlated. During REM, HD cells fired in structured patterns that encoded continuous orientation trajectories. In a large fraction of REM episodes, the decoded head direction exhibited trajectories with alternation profiles similar to those

observed during RUN. Moreover, heading trajectories were also correlated with hippocampal population activity. Our results demonstrate thalamic activity is temporally structured during REM and suggest that both thalamus and hippocampus simultaneously represent similar ambulatory states during REM. The strong similarity between thalamic activity during wake and REM raises the possibility that thalamic activity contributes to the rich sensory content that characterizes dream states.

## **Results**

### *HD cell activity during RUN*

To maximize the sampling of HD cell activity during RUN, rats ran on a circular maze. The track was partitioned by a high-wall divider to allow the definition of start and end points on either side of the wall. Rats shuttled back and forth between the start and end locations for food reward (Figure 1A). Consistent with previous reports, peak firing rates of recorded thalamic cells ranged between 13 - 100 Hz (Figure 1B). Only cells that could be identified during sleep and wake were included in the analysis. Ensembles consisted of five to nine units in four rats for a total of eight recording sessions.

RUN behavior was variable depending on the number of sessions each rat had been exposed to the track. To relate the firing of HD neurons to the rat's spatial behavior, we employed a Bayesian decoding algorithm (Zhang et al. 1998; Johnson, Seeland & Redish 2005). This approach allows us to estimate the orientation of the animal's head in time windows of arbitrary duration. Decoding

requires knowledge of two pieces of information about individual cells in the ensemble: the number of action potentials each cell fires in the decoding interval and the cell's average directional receptive field. Orientation estimation reports the likelihood associated with all possible orientations given the observed ensemble firing pattern. Estimation is expressed as a probability density function (PDF) over direction. By dividing the behavioral epoch into short duration windows we can reconstruct the heading trajectories that take place during task execution solely based on the activity of a set of HD cells (Figure 2A). Here we reconstructed heading trajectories using non-overlapping bins of 250 ms and 1 s durations. We started by assessing the capability of this decoding method to establish an association between ensemble firing activity and orientation behavior during RUN.

To evaluate the accuracy of the decoder, we calculated the estimation error in each time bin. Estimation error was measured as the difference between the mean tracked orientation and the estimated orientation with maximum likelihood (Figure 2C). Indicative of accurate reconstruction, estimation errors were only slightly larger when decoding with 250 ms bins (250ms bin, mean 21.06°, median 10.10°; 1s bin, mean 17.02°, median 8.50°;  $P < 0.001$ , rank-sum test) but within estimation resolution.

True head orientation varies continuously as a function of time. Since we partitioned RUN into independent bins, we were interested in assessing whether continuity was captured by the decoder. To this end, we calculated the distance between orientations with the highest estimated likelihood in consecutive estimation windows (Figure 2D). Median distances were lower when decoding at 250 ms resolution (250 ms bin, mean 24.74°, median 10; 1s bin, mean 32.57°,

median  $20^\circ$ ,  $P < 0.001$ , rank-sum test). Because rats may cover large fractions of orientation space in brief periods of time (Figure 2 A-B), differences in orientation between consecutive bins are expected to be larger when using partitioning the behavioral epoch with wider bins.

Having established that the decoding method adequately reflected actual heading trajectories, we used the mode from orientation PDFs to assess the correspondence in activity among HD cells during RUN. Note that, all other things being equal in an estimation window, the shape of the PDF and value of its mode change as a function of the internal consistency of firing among cells in the ensemble (Johnson, Seeland & Redish 2005). For instance, consider the scenario in which we want to estimate the rat's head orientation by observing two HD cells only. Assume their receptive fields are non-overlapping and are tuned to directly opposite directions. During the estimation window, if one cell fired and the other didn't, the estimator would predict the orientation to lie within the receptive field of the active cell only. However, if both cells were to fire within the decoding interval, the estimator would be unable to pick only one of the two directions without ambiguity. Instead, the estimator would indicate the possibility that the two directions can be associated with the firing pattern, albeit each with lower likelihood. The reduced certainty stems from the fact that cells in this example fire, on average, over orientation regions the animal could never face simultaneously. Thus, internally coherent firing ensembles result in estimations with higher certainty reflected by higher PDF mode values. At the other extreme, uncorrelated ensemble activities gravitate towards uniform likelihood estimations (peak probability value of 0.028 with  $10^\circ$  orientation resolution used here). Revealing internal consistency in ensemble activity during

RUN, the distributions of mode probabilities had median peak probability values significantly different from uniform distributions irrespective of bin size (250ms bin, median 0.44; 1s bin, median 0.76;  $P < 0.001$ , sign test). However, there was a tendency for estimations with 1 s bin to display tighter distributions (250 ms bin, mean 0.47, median 0.44; 1s bin, mean 0.73, median 0.76;  $P < 0.001$ , rank-sum test; Figure 2E).

We were interested in determining whether thalamic activity observed during RUN recurred during REM. One alternative would have been to search for estimated orientation sequences that matched those observed during RUN. Because HD cells signal the rat's current heading irrespective of ongoing behavior or location, a given heading sequence was not uniquely tied to particular events or track traversals during RUN. In light of this potential ambiguity, we set out to identify additional physiological features that characterized the spatial behavior of the rat more adequately. To this end, we investigated the relation between heading trajectories and two population measures: theta power and hippocampal multi unit activity (MUA). Theta rhythm is a large synchronous oscillation (5 - 12 Hz) conspicuous during exploratory behavior and REM (Vertes, Hoover & Prisco 2004). Theta has been observed in the extracellular local field potential (lfp) of several brain structures, including the hippocampus and anterior thalamic complex (Vertes, Albo & Prisco 2001). Theta is strongly modulated by the behavior of the animal and it provides a complementary, physiological tag to the experience of the rat during RUN (Figure 2A-B). In this study, we used theta recorded from thalamic tetrodes for our analysis because it consistently showed higher amplitude than theta

recorded from hippocampal tetrodes. In addition to theta, hippocampal MUA is also modulated by the ambulatory behavior of the rat (Fig 2A-B).

During RUN, rats alternated between periods of continuous heading changes and segments with mostly constant head orientations. Epochs with time varying orientations were characterized by increased levels in both hippocampal MUA and theta power. By contrast, stationary heading periods were distinguished by lower levels in MUA and theta power (Figure 2A). We quantified these observations by calculating cross-correlation coefficients at different lags between estimated angular velocity and theta or hippocampal MUA as follows: orientations were estimated using 1 s non-overlapping bins. A sliding window of 5 s duration (1 s step) was used to calculate the mean angular rate of change at each time point. The slope was calculated from the best linear fit to the observed direction estimates within the sliding window. Decoded orientations were smoothed with a Gaussian kernel ( $\sigma = 0.5$  s) prior to linear fitting. Binning and smoothing parameters were chosen to emphasize the broad modulation of orientation trajectories over the entire RUN epoch while suppressing millisecond scale variations (Figure 2A-B). Both, hippocampal MUA and mean theta power were calculated in 1 s non-overlapping bins. No smoothing was applied on either measure. Cross-correlograms were calculated between the magnitude of the estimated angular velocity and binned theta power or MUA. Cross-correlation series revealed peaks within 1 s lags (Figure 2F-G) for all rats. Since smoothing introduced a loss of independence between neighboring samples, we assessed the statistical significance of the correlation values in a way that explicitly incorporated the effects of smoothing. For each RUN session, we compared the observed peak correlation coefficients to sample distributions obtained from

shuffled version of the original spike data. We independently rearranged spike counts belonging to different cells to randomly assigned time bins, smoothed the resulting ensemble pattern and calculated the cross-correlations with the corresponding theta power or hippocampal MUA series. Monte Carlo p-values were  $< 0.001$  for all RUN sessions, indicating correlations were statistically significant.

### *HD cell activity during REM*

We identified REM episodes as sleep periods with elevated theta power, postural immobility, and no activity in neck electro myogram. Only epochs lasting at least 60 s were analyzed (N = 61, 28 before RUN, 33 after RUN; Figure 3G). We found no tendency to identify more REM episodes before or after RUN. However, a large proportion of REM epochs following maze running tended to appear at least one hour following RUN completion (Figure 3H).

Because during REM HD cells appeared to be active in a way that resembled their firing profiles during RUN, we tested the possibility that cell ensembles continued to encode heading trajectories during this sleep state. We decoded head orientations at 250 ms and 1 s resolutions (Figure 3A). We found that, in all analyzed epochs, thalamic activity was temporally structured to reflect continuous heading paths. The resulting trajectories were independent of bin size and replicated features present in orientation patterns decoded during RUN (Figure 3B). To evaluate RUN-REM similarities, we first assessed the degree of continuity in the decoded paths (Figure 3C). Replicating the observations during

wake, the median distance between neighboring directional estimations was within the decoding spatial resolution, irrespective of temporal binning. However, unlike RUN trajectories, the distribution of distances between neighboring estimations did not differ significantly when using 250 ms or 1 s bins during REM (250 ms bin, mean 28.28°, median 10°; 1 s bin, mean, 27.51°, median 10°;  $P = 0.08$ , rank-sum test). These results imply that orientation trajectories during REM were dominated by periods that changed at slower rates than during RUN.

Next, we assessed the internal activity consistency in the set of HD cells during REM (Figure 3D). We found the correspondence among HD cells during REM to be similar to their consistency during RUN. Indeed, maximum likelihood value distributions had median values that differed from uniformity with either decoding bin (250ms bin, median 0.45; 1s bin, median 0.81,  $P < 0.001$ , sign test). Much like RUN, estimations tended to be tighter with 1 s bin (250ms bin, mean 0.48, median 0.45; 1s bin, mean 0.77, median 0.81,  $P < 0.001$ , rank-sum test). When matching decoding bins durations we found a slight but significant tendency for estimations to have higher mode values during REM (250ms bin, RUN, mean 0.47, median, 0.44; REM, mean 0.48, median, 0.45; 1s bin, RUN, mean 0.73, median, 0.76; REM, mean 0.77, median, 0.81;  $P < 2.22 \times 10^{-16}$ ; rank-sum test). These results highlight the fact that internal coherence in ensemble activity is maintained across behavioral states.

The remaining question we wanted to address was whether the continuous orientation trajectories decoded during REM also replicated the relation between angular velocity and theta and MUA established during RUN. Reminiscent of

heading profiles during wake, the decoded REM trajectories included periods of continuous change along with epochs with constant orientations. We calculated cross-correlation at different lags between estimated angular velocity and the two population measures. Given that during RUN maximum correlations were found within one second lags, we restricted the cross-correlation analysis to include lags up to 2 s in either direction. Similar to the procedure used during RUN, we tested the statistical significance of the resulting peak correlations by comparing them to distributions of correlation coefficients observed after shuffling the original spike count data (Figure 3E-F). Out of 61 events, 28 (46%) showed a significant correlation (Monte Carlo p-value < 0.001) between angular velocity and theta power. Similarly, 25 events (41%) showed significant correlations to hippocampal MUA. Events with significant correlations were slightly more likely to be found before RUN (PRE, theta power, 15/28; MUA, 15/28; POST, theta power, 13/33; MUA, 10/33). About 75% of the significant events detected after RUN tended to happen between 1.5 to 3 hours following maze running (Figure 3H).

#### *Comparison to place cell activity during REM*

An interesting question raised by the above correlations is whether there exists a correspondence at finer time scales between hippocampal and thalamic activity. Specifically, it has been demonstrated that during REM, place cell activity in the hippocampus is temporally structured to reflect previous experiences (Louie & Wilson 2001). Similar to the findings described here, hippocampal replaying REM events were reported to reproduce theta power

variations observed during execution of the spatial task. We were interested in assessing whether orientation trajectories encoded by thalamic ensembles were consistent with the spatial content of hippocampal place cell activity during REM. To address this possibility, we simultaneously recorded the activity of hippocampal place and thalamic HD cells in three out of four rats, for a total of six sessions. Place cell ensembles consisted of 18 – 35 cells. To compare the spatial content of hippocampal cells with that of thalamic ensembles, we reconstructed head orientations based on the activity of place cells (Figure 4A-B). First, we verified that heading trajectories during RUN could be successfully reconstructed by hippocampal spiking activity using 250 ms and 1 s duration bins. Similar to thalamic-based decoding during maze running, median estimation errors were within the decoding spatial resolution during periods of active locomotion. Estimations had a slightly larger error with 1 s bins (250ms bin, mean 26.55°, median 8.84°; 1s bin, mean 20.85°, median 9.16°;  $P = 0.048$ , rank-sum test; Figure 4C). Next, we evaluated the correspondence between HD and place cells during REM episodes with significant correlations between thalamic-based estimated angular velocity and theta power. We carried out this part of the analysis with data from 1s decoding bins. We fragmented REM events distinguishing two event categories based on thalamic spatial content: periods of constant orientations or epochs displaying time varying heading trajectories (Figure 5A). Only epochs lasting more than four seconds were included. This duration threshold yielded 95 stationary periods and 106 epochs with time varying head orientations. When HD spiking activity indicated stationary orientations, place cells also tended to encode constant directions (Figure 5B, left). To quantify this observation we identified the best linear fit to

the orientation estimations from HD and place cell ensembles. Over 60% (58 out of 95) of the events in which thalamic-based orientations displayed slopes within  $\pm 5^\circ/s$ , hippocampal-based directions were best described by lines with slopes bound within  $\pm 8^\circ/s$ . Although both brain areas reflected constant orientations, there was no systematic relationship between the directions they encoded.

The thalamic-based time varying orientation profiles exhibited clear trajectories that could not be accurately described by linear fits. By contrast, hippocampal-based orientations did not always yield clear, uninterrupted trajectories. However, the decoded directions tended to span wide ranges of orientation space. Importantly, the range of orientations encoded by both cell groups appeared to be comparable (Figure 5B, left). We quantified this observation by calculating the range of direction estimations by the two cell groups. Orientation ranges exhibited a small but significant correlation (0.28,  $p = .025$ ). In summary, our data showed a tendency for place and HD cells to simultaneously reflect similar ambulatory states during REM.

## **Discussion**

Current knowledge about the anatomy and electrophysiology of the thalamus points to a prominent role in the regulation of information flow to cortical areas. Despite the established distinction in transfer of information between wake and SWS, the role of thalamic activity during REM remains unknown. On the basis of increased cell excitability from SWS to REM, it has been suggested that the

thalamus could be actively involved in ongoing internal processes during the latter sleep stage (Hirata & Castro-Alamancos 2010). We hypothesized that thalamic activity recreates sensory representations encoded during awake behavior. Compatible with this view, here we show that during REM, ensemble activity from thalamic HD cells is temporally structured to represent heading trajectories with remarkable similarities to the orientation paths encoded during active exploration. Moreover, the corresponding estimated angular velocity reproduces relationships with other physiological measures that characterize different ambulatory states during RUN.

#### *Continuity of heading trajectories during REM*

Our analysis involved the use of a neural estimation algorithm, which allowed us to interpret the spiking activity of thalamic ensembles in terms of a spatial correlate. This method revealed several features of thalamic activity that paralleled those characteristic of awake behavior. One of the most striking similarities between REM and RUN was the presence of continuous heading trajectories throughout the duration of individual sleep episodes. Note that the implementation of the estimation algorithm used in this study involved segmenting the spiking activity into decoding bins. To what extent did the choice of binning parameters influence the emergence of heading trajectories? To answer this question we employed non-overlapping decoding windows of different durations, namely 0.25 and 1 s. Trajectories were qualitatively similar using either window demonstrating the robustness of our finding. However, there were quantitative differences when using the two decoding bin sizes.

Specifically, mode values from the estimation PDFs increased when using 1 s bins, reflecting greater estimation certainty with the longer duration window. Importantly, the difference in mode value distributions between 0.25 and 1 s bins was also evident during RUN. Indeed, when comparing the distributions of PDF peak values between RUN and REM, no statistical difference was found when matching the duration of the decoding bins. It is important to highlight that mode values provide an opportunity to evaluate the correspondence in activity among cells of the ensemble. The similarity in mode distributions between RUN and REM reveals that thalamic cells continue to exhibit an equal level of coordination in activity at the network level during REM sleep.

#### *Correlation between angular velocity and population activity measures during RUN and REM*

Continuity of heading trajectories during REM is a necessary, but not sufficient, condition to demonstrate that HD cells recreate activity related to RUN behavior. The limitation arises from the fact that HD cells fire in relation to the orientation of the animal irrespective of position or behavior. Since in our experiments animals were able to freely move their heads, a given orientation profile could not be uniquely associated with particular behaviors or events on the maze. A key element used in the design of our experiment to overcome this ambiguity is the well established correlation between theta power, or hippocampal MUA, and active locomotion. Both physiological measures increase as a function of movement speed. In our task, rats ran back and forth between two points on a circular track, where they paused to receive food reward. Execution of the task

imposed a direct association between theta power, hippocampal MUA and angular velocity. This relationship allowed us to identify REM episodes in which alternations in angular velocity concurred with alternations in theta power and MUA, replicating the overall characteristic structure of RUN. It is important to note that the identification analysis involved a smoothing procedure applied to the decoded orientation profiles followed by a measure of correlation with either population variable. An undesirable consequence of smoothing is that it can artificially introduce correlations between otherwise independent variables. We addressed this issue by assessing the statistical significance of our correlation measure with the use of a shuffle procedure that directly tested the effect of smoothing. Specifically, for each REM episode, we independently randomized the position of spike count bins for each cell. We reasoned that the resulting correlation coefficients should be mainly attributable to smoothing because shuffling disrupts the original spatio-temporal structure within the cell ensemble. By choosing a conservative significance threshold value ( $p < 0.01$ ) we minimized the possibility of erroneous classification.

Previous work on hippocampal place cells identified significant representations of familiar trajectories during REM, with most correlations occurring 24 hours following exploration of the maze. An unresolved question in that study was whether their observation was the result of a slow rate at which mnemonic information is incorporated into REM or simply reflected a difference in sleep quality between REM before and after RUN. Here we identified REM activity corresponding to RUN in both, sleep immediately following, and 24 hours after, awake behavior. Importantly, most significant correlations in REM following RUN occurred between 90 minutes and three hours after a session on the track. This

observation suggests that information is re-expressed, at least in thalamic circuits, within a few hours after the end of spatial training and it continues to be present for at least 24 hours.

*Similar ambulatory states represented by thalamus and hippocampus during REM*

An important finding common to hippocampal reactivation and our work here is the reproduction of modulations in theta power in conjunction with ensemble spiking activities. Given the similarities in the two studies, we directly evaluated the correspondence between hippocampal and thalamic activities at a higher temporal resolution during REM in a subset of animals. We found a consistent co-representation of ambulatory states in both brain areas, albeit with different directional content each. Specifically, when thalamic neurons represented constant orientations, place cells tended to also encode stationary directions. However, the decoded orientations in the two structures were uncorrelated. Similarly, when thalamic cells represented active heading trajectories, hippocampal activity displayed noisy or discontinuous trajectories, which did not necessarily match the corresponding thalamic representations. Two observations deserve further consideration here: the apparent weaker spatial representation by hippocampal activity during the presumed active portions of REM and the coincident ambulatory state but discordant spatial representations between HD and place cells. The former observation is in contrast with the previously reported specificity in hippocampal firing patterns between RUN and REM (Louie & Wilson 2001). What could be the cause of the current weaker

spatial representation by hippocampal cells? One contributing factor might involve the methodology used in our study. Successful decoding of a particular position at a given time requires the simultaneous spiking of cells with overlapping place fields at that location each in proportion to its in-field firing rate. In addition, neurons with receptive fields in other regions of the maze must be simultaneously inactive. Violations of either requirement give rise to broader spatial estimations which, in turn, lowers the strength of the spatial representation. In light of these requirements, it is likely that sparse hippocampal firing during REM might be the dominant contributor to the weakened spatial representation. When attempting to reconstruct an orientation trajectory the effect is manifested either as a noisy curve or as a heading path with frequent discontinuities. By contrast, a template-based correlation measure reflects the relative similarity between two spatio-temporal activity profiles and therefore is more robust against the effects of irregular firing. Hence, it is possible that patterns with significant matches obtained from template correlations would also translate into noisy spatial representations with our estimation method.

A second factor that should be considered is the possibility that the behavioral demands during spatial tasks have a direct impact in the subsequent hippocampal content during REM. How would behavior influence the spatial representation of future replay events? Louie & Wilson (2001) pondered that a potential mechanism for extended hippocampal replay might come about from interactions between prefrontal and hippocampal circuits during REM. Interestingly, dual recordings in the dorsal prefrontal cortex and hippocampus have shown transient increases in coherence between the two structures during

periods of increased working memory load in spatial navigation tasks (Jones & Wilson 2005; Siapas, Lubenov & Wilson 2005). A potential consequence of such coordination would be the temporary synaptic strengthening between cortical and hippocampal neurons which could then be reflected during REM replay events. Consistent with this notion, Louie & Wilson (2001) employed a task in which rats needed to remember the most recently rewarded position and, based on that information, identify the location of the next target site. Their task would be expected to engage coordinated activity in prefrontal and hippocampal circuits given its mnemonic and decision making elements. By contrast, in the present study we employed a barrier that passively directed animals towards the next rewarded point on the maze effectively removing mnemonic or decision making components during locomotion. Consequently, little or no coordination between prefrontal and hippocampal activities would be expected during this phase of the task. If coherence between prefrontal and hippocampal areas during wake has an effect on hippocampal REM replay, it is conceivable that the data of Louie & Wilson (2001) and our data would display different degrees of spatial correspondence between RUN and REM. Ultimately, the extent to which hippocampal REM replay reflects, or is otherwise biased by, awake cortico-hippocampal interactions requires additional investigation.

Lastly, an interesting possibility is that the content displayed by the current hippocampal ensembles reflects neuronal configurations corresponding to other behavioral experiences in which heading trajectories also show alternation profiles. Particularly, rats in our study were exposed to a circular track in a secondary room where spontaneous alternations were rewarded. This training period lasted about a week and did not overlap with the data collection period.

An important characteristic of HD cells is that while they may switch preferred orientations in different environments, their relative orientation preferences remain unchanged (Taube & Burton 1995). Consequently, if the spatial representation by HD cells during REM corresponded to the prior training experience, features such as trajectory continuity and ensemble consistency would be preserved. However, decoded heading trajectories would differ from those decoded here by a constant offset. By contrast, the relationship between place cells in different environments is mostly unpredictable (Leutgeb et al. 2005a). As a consequence, the cell ensembles we monitored during recording might only partially overlap with cells that were active on the training maze. As a result, the spatial representation during REM would be detrimentally affected should hippocampal activity be related to the previous training exposure. This scenario would account for the observation that thalamic and hippocampal representations agree in ambulatory state representation but not in their specific spatial content.

### *Potential Mechanisms*

What mechanisms could give rise to the structured activity in thalamic HD cells? Anatomically, the anterior thalamus is embedded within an extensive network of interconnected structures including the hippocampus with which it shares reciprocal connections. Given place cell reactivation during REM, it is conceivable that the hippocampus might engage the anterior thalamus via its fornix projections. Our data provide only weak support for direct communication between these areas given the unexpected mismatch in directional content

between HD and place cells during REM.

An alternative avenue for communication between the anterior thalamus and hippocampus is provided by the retrosplenial cortex. In addition to being reciprocally connected with these structures, the retrosplenial cortex also communicates with discrete areas of the dorsal prefrontal cortex (Vann, Aggleton & Maguire 2009). Echoing the proposal by Louie & Wilson (2001), both hippocampal and thalamic activities during REM could result from prefrontal influences in each area. In this case, the retrosplenial cortex could serve as a common modulator of activity to thalamic and hippocampal networks.

The finding that theta power modulation and heading trajectories are also co-expressed during REM raises the possibility that subcortical inputs could mediate such co-activation. In particular, it is well established that cholinergic cells from the pedunculo pontine and laterodorsal tegmental (PPT/LDT) nuclei have a direct influence in the activities of several brain areas during REM (Steriade 2004). Specifically, PPT is involved in the generation of theta (Vertes, Hoover & Prisco 2004), while PPT and LDT bring virtually all thalamocortical cells closer to their firing threshold during REM. It is important to note that while cells in the anterior thalamus can exhibit strong theta modulation, the majority of those neurons are located in the ventral subdivision and are not modulated by the spatial orientation of the animal (Vann & Aggleton 2004; Vann, Saunders & Aggleton 2007). Indeed, theta modulated and HD cells in the anterior thalamus form parallel streams of information with little interaction between them until after they reach the hippocampal formation. This segregation suggests that cholinergic activity might act as a facilitator of activation rather than as a direct driver of activity on HD cells during REM.

Overall, our results are consistent with the notion that thalamic cells are engaged in a global recapitulation of the awake state during REM. Particularly, the coincident representation of ambulatory states by HD and place cells might provide spatial context that could be used by other brain structures involved in the integration of spatial information and route planning. This information could be used for the formulation or evaluation of alternative routes. At the same time, the expression of discordant orientation trajectories by hippocampal and thalamic ensembles might be directly associated with the ubiquitous presence of confabulatory events that characterize dream states.

## **Methods**

### *Electrophysiology*

Four male Long-Evans rats (500 – 600 g) were implanted with arrays of 18 independently movable tetrodes. Six tetrodes were aimed at the anterior dorsal thalamus (ADN; -2.1 mm AP, 1.3 mm ML, relative to bregma) and the remaining 12 tetrodes to the CA1 layer of the dorsal hippocampus (CA1; -3.6 mm AP, 2.1 mm ML, relative to bregma). A bipolar electrode was inserted in the neck muscle to record electromyographic (EMG) activity. Surgical procedures and behavioral testing were approved by the Committee of Animal Care at Massachusetts Institute of Technology and followed US National Institute of Health guidelines.

After implantation, tetrodes were advanced over the course of several days until they rested near the target areas. After the initial positioning, the depth of

individual tetrodes was adjusted to increase unit yield. To maximize signal stability, recordings took place at least 12 hours following the last depth adjustment. Spikes crossing a preset threshold on any of the four leads of a tetrode were recorded at 32 kHz for subsequent analysis. A custom written software (Xclust, M.A.W) was used to identify and isolate individual cells based on spike amplitude and waveform. Multi unit activity (MUA) was defined as the set of spikes with a minimum amplitude of 70  $\mu$ V on any of the four wires of a tetrode. Local field potential (LFP) and EMG signals were bandpass filtered between 1 - 475 Hz and sampled at 2 kHz. Position and head direction were measured by a pair of diode arrays mounted on the head-stage and aligned with the long axis of the rat. Sampling took place uninterruptedly at 30 Hz by an overhead camera.

### *Behavioral Procedures*

During the initial tetrode positioning period, rats were exposed to an elevated circular track in a secondary room to encourage exploratory activity. Rats were rewarded for spontaneous alternations between clockwise and counterclockwise trajectories. Data acquisition took place in a different room and on a novel maze about a week after the last exposure to the training track. In the new task, rats ran back and forth between two points on either side of a high wall divider attached to the elevated circular maze (125 cm diameter, 10 cm width; Figure 1A). Food reward was given when the rat successfully traversed the entire track to reach the food well. No behavioral criterion for task performance was required. A typical experimental session involved 1 - 3 hr sleep epochs before

(PRE) and after (POST) a 25 - 35 min period of active exploration (RUN). Both sleep sessions were conducted on an elevated dish within a high walled enclosure away from the maze. The sessions reported here correspond to days in which at least 5 head direction cells were recorded and are not necessarily matched for each rat's familiarity with or running performance on the track.

### *Receptive fields*

One dimensional place tuning was measured on linearized coordinates. Linearization took place by transforming each point's Cartesian coordinate (x,y) to its corresponding polar coordinate ( $\rho, \theta$ ), where  $\theta$  was measured relative to the line joining the circle center and an arbitrarily selected starting position on the track. The angle coordinate was then transformed into distance units by determining the length of the arc it described on a circle with a 62.2 cm radius. Position (head direction) tuning was quantified by counting the number of spikes fired in non overlapping 10 cm (10 deg) bins and dividing them by the total amount of time the rat occupied (faced in the direction specified by) each bin. Only spikes fired when the rat had a linear speed  $> 15$  cm/s were used for calculation of hippocampal receptive fields. All spikes, irrespective of linear or angular velocity, were used to assess the directional tuning of thalamic cells.

### *Position/Head direction Decoding Analysis*

We used a Bayesian decoding algorithm to estimate position (head direction) in non overlapping time bins based on the activity of cell ensembles (Zhang et al.

1998; Johnson, Seeland & Redish 2005). Estimation returns the likelihood with which the observed ensemble firing profile could be associated with each position (head direction) and is given by:

$$P(\mathbf{x}|\mathbf{n})=C(\tau,\mathbf{n})P(\mathbf{x})\left(\prod_{i=1}^N f_i(\mathbf{x})^{n_i}\right)\exp\left(-\tau\sum_{i=1}^N f_i(\mathbf{x})\right) \quad (1)$$

where  $C(\tau,\mathbf{n})$  is a normalization factor,  $P(\mathbf{x})$  represents the position (head direction) prior probability,  $f_i(\mathbf{x})$  is the receptive field of the  $i$ th recorded cell and  $n_i$  are the number of spikes fired by the  $i$ th cell in the observation window of duration  $\tau$  (0.25 or 1 s used here). Prior probabilities for position and head direction were assumed to be uniform. Use of bold notation for  $\mathbf{x}$  and  $\mathbf{n}$  stresses the fact that estimation likelihood is expressed for the range of all possible values the spatial variable can take and that its calculation takes into account the simultaneous activity of the  $N$  recorded cells.

Decoding errors were quantified by choosing the estimation with maximum likelihood and comparing it to the mean value of the spatial variable during the estimation time bin. Differences in estimation errors during different behavioral epochs or decoding bin sizes were tested statistically by means of the rank-sum test.

### *Angular Velocity - Theta Power Correlation Analysis*

Angular velocity was calculated from estimated heading trajectories with a 5 s sliding window (1 s step). At each time step, the best linear fit to the decoded orientation profiles was determined by finding the line that maximized the mean

estimated likelihood in that window (Toft 1996). The corresponding slope was assigned to that time point as its angular velocity. Decoded orientations were smoothed with a Gaussian kernel ( $\sigma = 0.5$  s) prior to linear fitting. Theta power was calculated in 1 s non-overlapping intervals. Lfp traces were filtered in the theta range (5 - 12 Hz) and the tetrode with the greatest signal amplitude was used to compute the root mean square value. Mean MUA was calculated as a linear average in the same time bins and included data pooled across all hippocampal tetrodes. Cross-correlation coefficients at time lag  $\Delta t$  were calculated as

$$C_{AngVel,\theta}(\Delta t) = \frac{\sum_{t=1}^n (f_{AngVel}(t) - \overline{f_{AngVel}})(g_{\theta}(t+\Delta t) - \overline{g_{\theta}})}{\sqrt{\sum_{t=1}^n (f_{AngVel}(t) - \overline{f_{AngVel}})^2} \sqrt{\sum_{t=1}^n (g_{\theta}(t) - \overline{g_{\theta}})^2}} \quad (2)$$

where

$$\overline{f_{AngVel}} = \frac{1}{n} \sum_{t=1}^n f_{AngVel}(t) \quad (3)$$

$$\overline{g_{\theta}} = \frac{1}{n} \sum_{t=1}^n g_{\theta}(t) \quad (4)$$

and  $f_{AngVel}$  and  $g_{\theta}$  are functions that represent the magnitudes of the angular velocity and theta power or MUA, respectively. The statistical significance of the correlations was assessed by comparing them to sample distributions resulting from a shuffled versions of the original spike count data in which the spike times of each cell were independently rearranged in a random fashion.

### *Sleep classification*

REM sleep was identified as periods of increased theta power during the intervals rats spent in the sleep box. Epochs in which the theta to delta ratio exceeded its mean value by one standard deviation were initially considered as potential REM events. In addition, we verified that EMG activity was below its mean value and that rats' position and orientation remained constant. Candidate REM epochs separated by brief (up to 10 s) gaps were grouped into single events as long as the rats' posture did not change during the entire REM period and no increase in delta (0.5 - 4 Hz) could be detected.

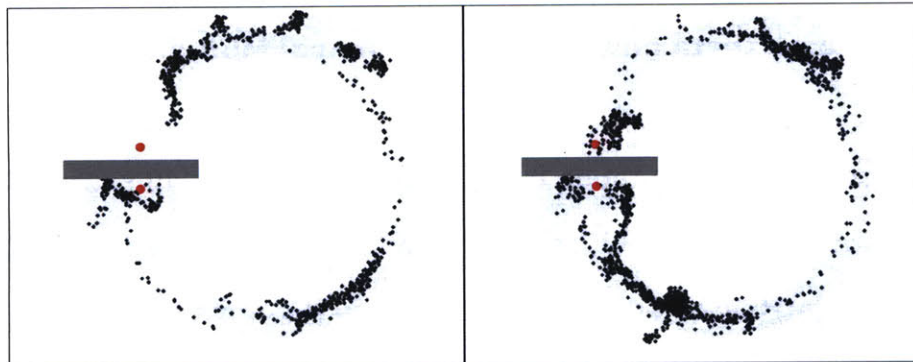


**Figure 1. Behavioral task and receptive fields of thalamic HD cells.**

(A) Data from one rat showing cumulative position records (light gray) during 26 minutes of RUN behavior on a circular track. Rats ran back and forth between end points of the track (red circles) for food reward. Dark-gray rectangle indicates high-wall barrier attached to the track. Black dots represent spikes fired by HD cells with preferred orientations at  $50^\circ$  (left) and  $-40^\circ$  (right) during two consecutive laps. Note that, as a consequence of uninterrupted running, each position on the track became associated with a narrow range of orientations during RUN. Consequently, the spiking activity of HD cells appears to be associated with selected locations.

(B) Receptive fields of six HD cells (black bars) normalized by orientation occupancy. Receptive fields were calculated during RUN with a  $10^\circ$  bin size. Firing rates at preferred orientations are indicated in each panel.

A



B

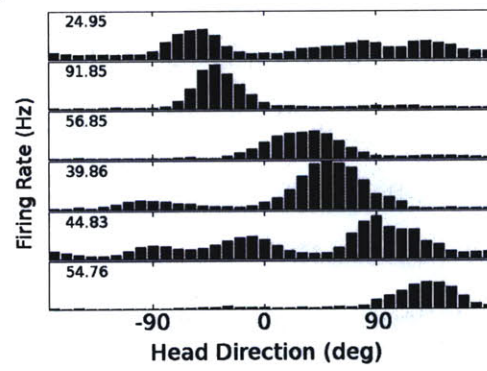


**Figure 2. Angular velocity estimated from thalamic cell activity is correlated with theta power and hippocampal MUA during RUN.**

(A-B) Decoded head orientation over three minute (A) or 40 second (B) periods during maze running for rat1, session 1. Top two panels display average tracked (red) and estimated (gray) head direction using 250 ms (top) or 1 s (bottom) decoding windows. Estimated likelihoods are expressed as probabilities linearly mapped between white (0) and black (1) colors. Estimation is based on the spiking activity of six HD cells whose receptive fields are shown in Figure 1. Cell firing is depicted in middle panel. Each tick mark represents an action potential and each row corresponds to a different cell. Bottom two panels show hippocampal MUA (top) and mean theta power (bottom) signals which were quantified in 1 s non-overlapping bins.

(C) Distribution of orientation estimation error for 250 ms (left) or 1 s (right) decoding bins for data in (A). Estimation error was calculated as the difference between mean tracked head direction and estimated head orientation with maximum likelihood. Median errors (9.71, 250 ms bin; 8.25, 1 s bin) are indicated by red dashed lines.

(D) Distribution of orientation distances between consecutive estimations for 250 ms (left) or 1 s (right) decoding bins (data from A). Estimation with 1 s bin introduced a slight shift towards higher increments between adjacent bins. Median distances (10°, 250 ms bin; 20°, 1 s bin) are indicated by red dashed lines.

(E) Distribution of PDF mode value for 250 ms (left) or 1 s (right) estimation bin. Mode value for uniform distribution indicated by green dashed lines. Estimation with either bin resulted in non-uniform PDFs. Decoding with 1 s bin biased estimation likelihood to higher probability values. Median PDF mode values (0.5, 250 ms bin; 0.8, 1 s bin) are indicated by red dashed lines.

(F-G) Cross-correlation series between estimated angular velocity and theta power (F, left) or hippocampal MUA (G, left). Cross-correlation was computed at different delays with theta power or hippocampal MUA as the reference signal. Angular velocity was calculated using estimated orientations at 1 s resolution. Statistical significance was assessed by comparing the observed peak correlation coefficient to sample distributions obtained from shuffled versions of the original spike count (right columns of F and G).

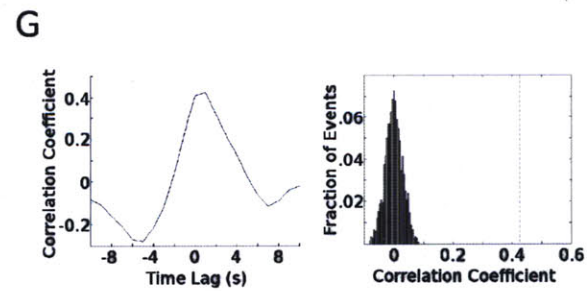
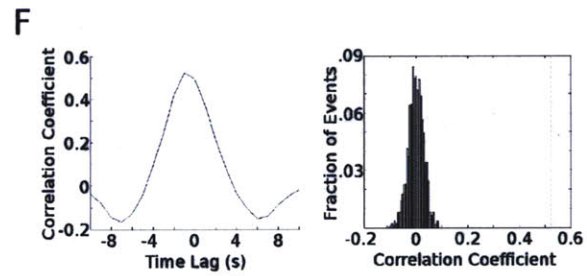
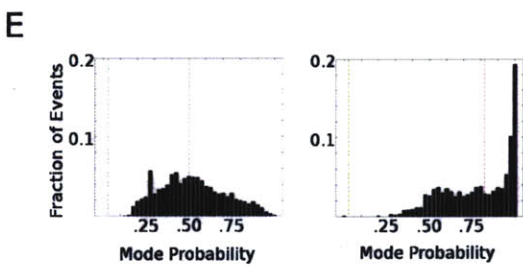
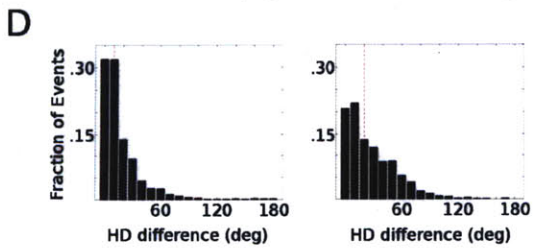
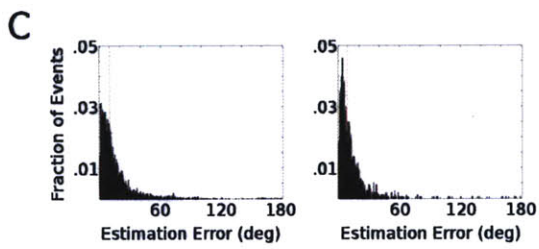
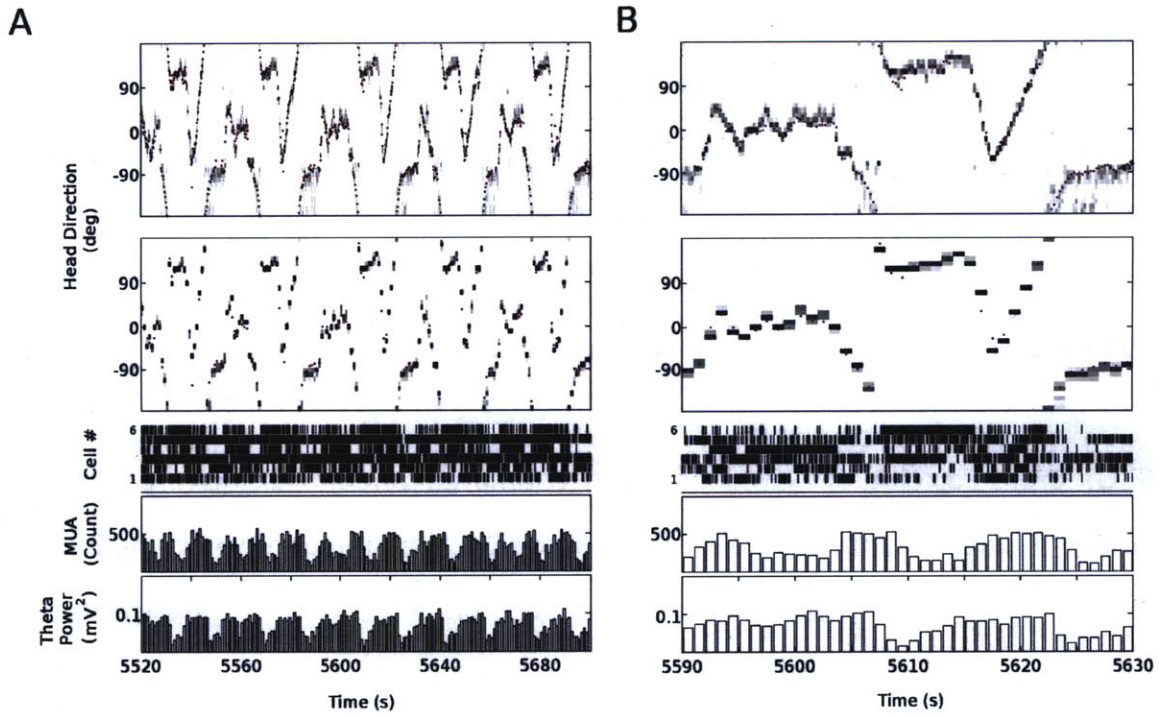


**Figure 3. Thalamic ensembles encode continuous orientation trajectories that are correlated with theta power and hippocampal MUA during REM.**

(A-B) Estimated orientation over a 120 second REM episode (A) or 110 second RUN period (B) for rat2, session 1. Top panels display average tracked (dashed line or red circles) and estimated (gray) head direction using 250 ms (top) or 1 s (bottom) decoding windows. Estimation is based on the spiking activity of seven HD cells whose activity is displayed in middle panel. Bottom two panels display the corresponding hippocampal MUA (top) and mean theta power (bottom) signals, which were quantified in 1 s non-overlapping bins.

(C) Distribution of orientation distance between consecutive estimations for 250 ms (left) or 1 s (right) decoding bins during REM episode shown in A. Median distances ( $10^\circ$ , 250 ms bin;  $10^\circ$ , 1 s bin) are indicated by red dashed lines.

(D) Distribution of PDF mode value using 250 ms (left) or 1 s (right) estimation bins for REM episode shown in A. Mode value for uniform distribution indicated by green dashed line. Median mode value shown as red dashed lines.

(E-F) Assessment of statistical significance of peak cross-correlation coefficient between estimated angular velocity and theta power (E) or hippocampal MUA (F) for REM episode shown in A. Dashed lines represent observed peak cross-

correlation coefficients. Bars correspond to sample distributions obtained from shuffled versions of the spike count data.

(G) REM episode duration as a function of time relative to RUN. Gray dashed line indicates threshold duration (60 s) above which REM episodes were analyzed.

(H) Cumulative distribution of REM episodes detected following RUN. Gray line corresponds to REM episodes lasting at least 60 s. Dotted red line corresponds to episodes with a significant correlation to theta power. Dashed red line corresponds to events with significant correlation to hippocampal MUA.

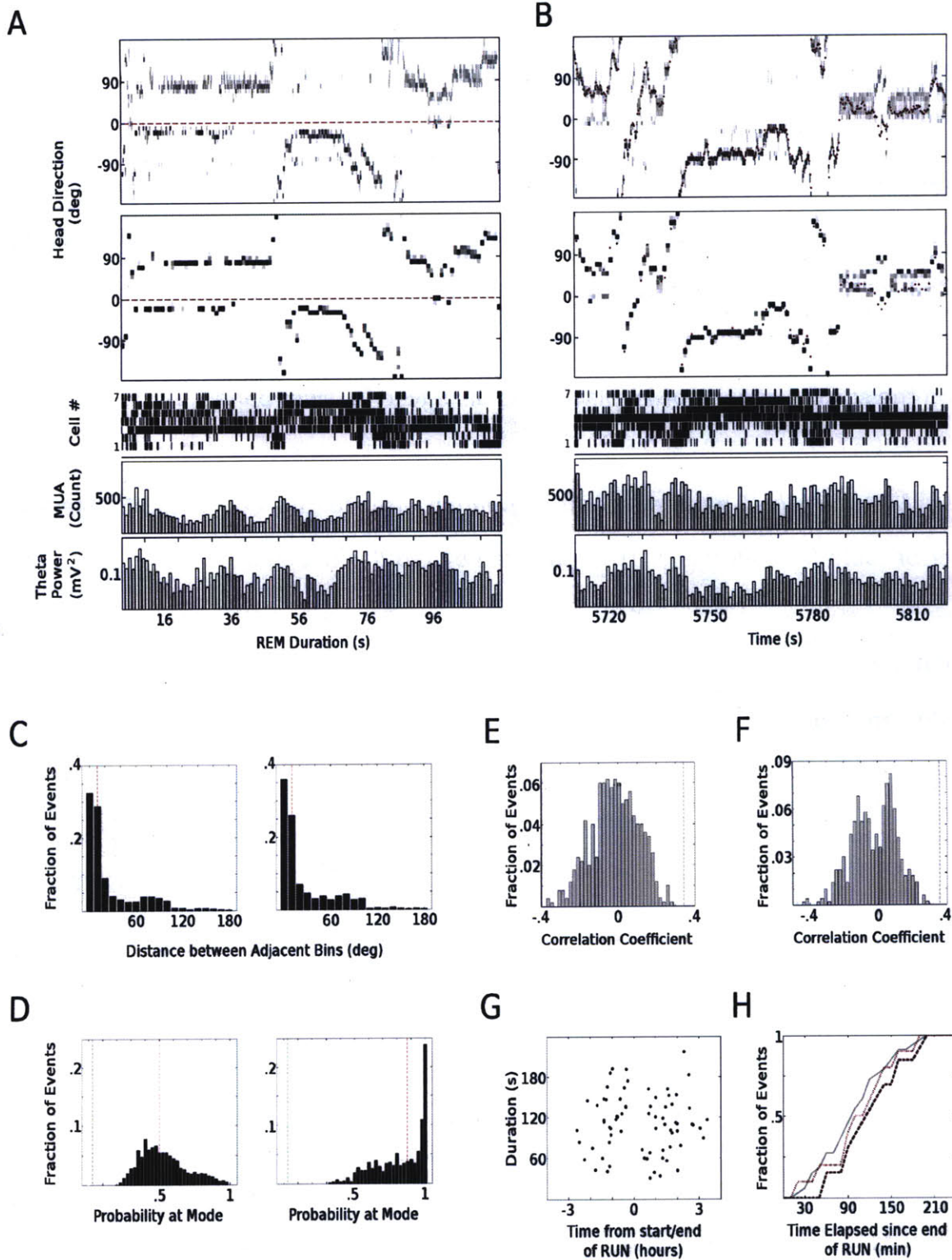
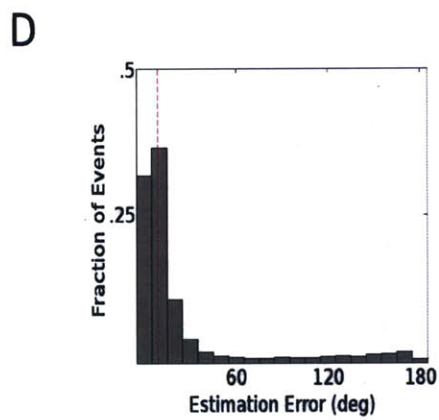
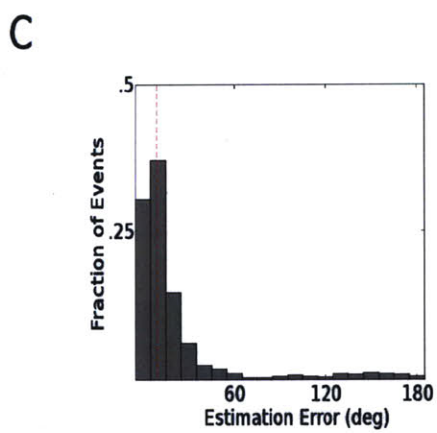
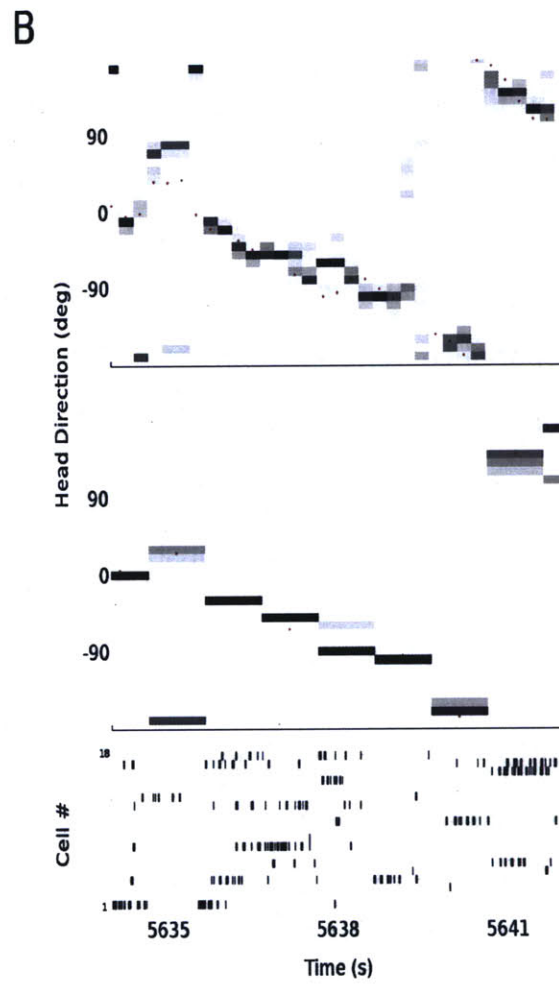
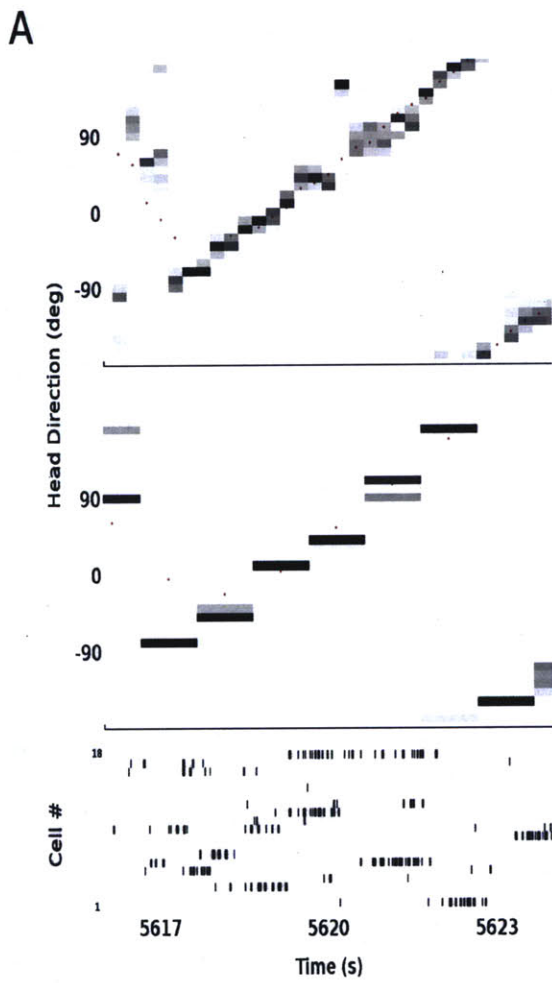


**Figure 4. Estimated orientation based on spiking activity of hippocampal place cells during RUN.**

(A-B) Decoded head direction over eight second periods during maze running. Top panels display average tracked (red) and estimated (gray) orientation using 250 ms (top) or 1 s (bottom) decoding bins corresponding to clockwise (A) or counterclockwise (B) heading trajectories for rat1, session 1. Estimation is based on the spiking activity of 18 place cells displayed in lower panels.

(C) Distribution of head direction estimation error for 1 s decoding bin. Median error (data from all rats,  $9.16^\circ$ ) indicated by red dashed line.

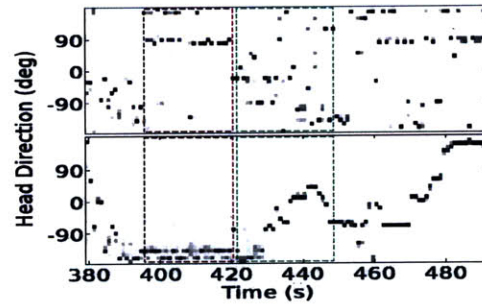
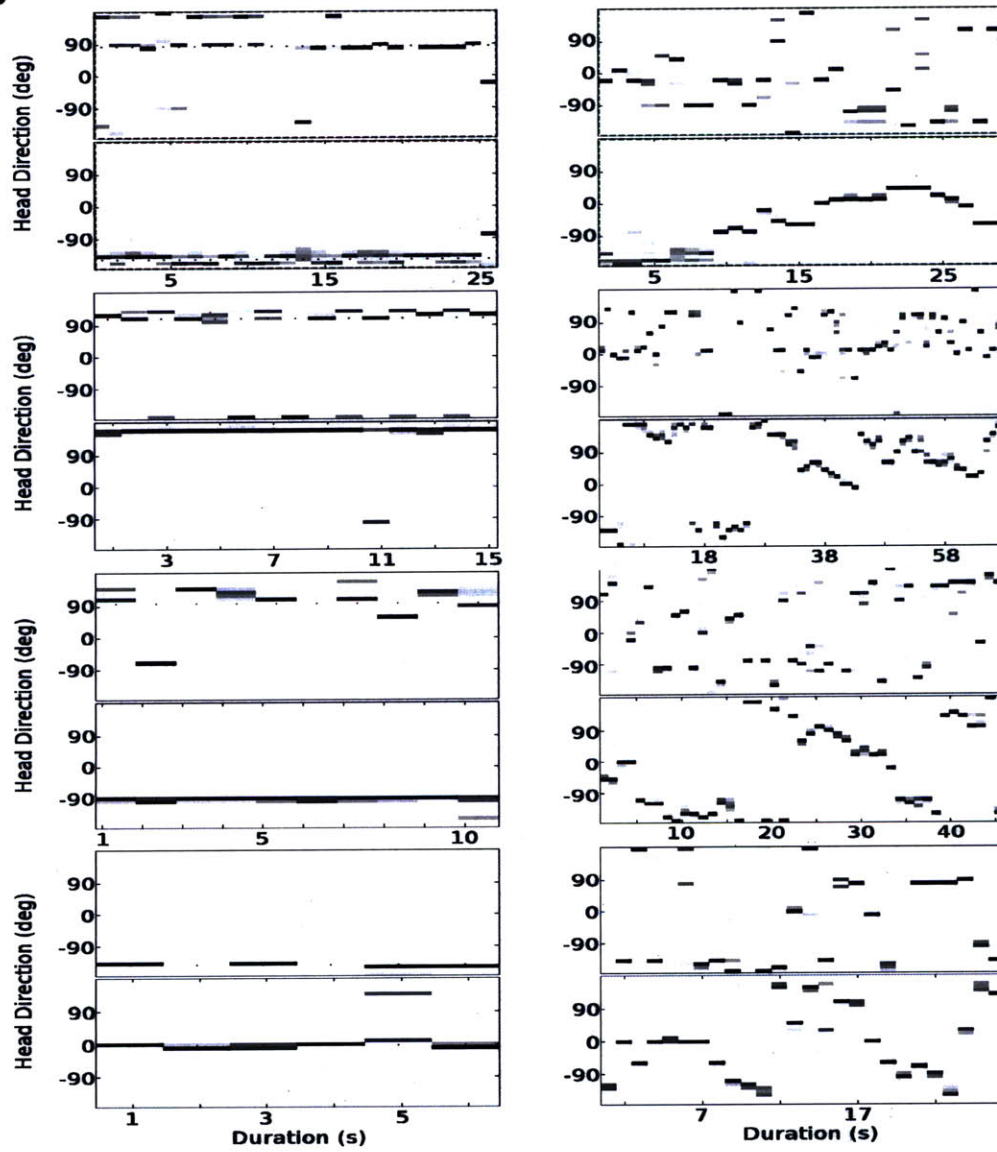
(D) Distribution of head direction estimation error for 250 ms decoding bin. Median error (data from all rats,  $8.84^\circ$ ) indicated by red dashed line.



**Figure 5. Comparison between estimated orientation based on hippocampal and thalamic cell spiking activities during REM.**

(A) Estimated head orientation by ensemble activity of hippocampal place cells (top) or thalamic HD cells (bottom) during a 105 s REM episode. Comparison of spatial content between structures was restricted to REM events with significant correlations between thalamic activity and theta power. Within each REM event, we distinguished two cases based upon decoded orientations from thalamic activity: Periods with constant (red box) or time-varying orientations (green box).

(B) Examples from three rats in four different recording sessions. Left column corresponds to segments with stationary orientations. Right column corresponds to periods with changing head direction. Top panels display hippocampal-based decoding. Bottom panels depict thalamic-based decoding.

**A****B**



## **Chapter 4**

### **Summary and Conclusions**

The main focus of this thesis was to further characterize the relationship between the hippocampus and anterior thalamus during different behavioral states in the rat. To this end, we designed a simple behavioral task in which we could simultaneously monitor the activity of thalamic head direction (HD) and hippocampal place cells during periods of navigation and sleep. We distinguished and analyzed four different behavioral states, namely: active locomotion, awake immobility, slow wave sleep (SWS) and rapid eye movement sleep (REM). We utilized a neural decoding algorithm (Zhang et al. 1998; Johnson, Seeland & Redish 2005; Davidson, Kloosterman & Wilson 2009) to establish the spatial content in ensembles of well isolated cells during awake behavior and REM. This approach provided common grounds for quantitative comparison between the activities of the two different structures.

In Chapter 2, we explored whether, during awake behavior, the spatial representations provided by hippocampal and thalamic cells remain correlated irrespective of locomotor activity. This question was motivated by the notion that HD and place cells underlie the subjective sense of direction and location, which are thought to be fundamental components of navigation. Consistent with this idea, we found that place and HD cells represented location and heading information with great accuracy during active locomotion. However, during hippocampal awake replay the activities of HD and place cells were decoupled. Because the present task introduced a correlation between the position and orientation of the animals on the track, we asked whether HD cells would encode the corresponding orientation sequence during hippocampal replay. We found that not to be the case. Instead, HD cells continued to signal the current head orientation of the animals uninterrupted. This finding is interesting

because it highlights the fact that internal representations of location and direction are supported by networks of cells that can act in a synergistic or independent manner according to behavioral or cognitive demands. In this regard, recent findings suggest that awake replay might underlie the manifestation of all potential routes available to the animals during navigation (Gupta et al. 2010). Our finding suggests that the evaluation of such routes does not involve directional information encoded by HD cells.

In the second part of Chapter 2, we studied the relationship that exist between the anterior thalamus and hippocampus during SWS at the population level. The characterization of MUA patterns was motivated by the idea that hippocampal replay during sleep contributes to the consolidation of episodic memories. Recent studies in rats support this notion by demonstrating that the acquisition of navigational tasks are slowed down by the selective interruption of ripple events during SWS (Ego-Stengel & Wilson 2009; Girardeau et al. 2009). A proposed mechanism for the consolidation of memories involves the transfer of information to extrahippocampal sites (Buzsáki 1989). In this respect, cortical areas have been shown to be correlated with hippocampal activity at the population and cell ensemble levels (Siapas & Wilson 1998; Ji & Wilson 2007). Given the well characterized corticothalamic interactions during sleep, we investigated whether thalamic and hippocampal activities are also correlated during SWS. We found that hippocampal MUA bursts tend to occur about 90 - 100 ms before and after thalamic MUA bursts raising the possibility of bidirectional communication between thalamus and hippocampus.

We were also able to establish that, during SWS, thalamic activity is organized in alternating patterns of depolarized and hyperpolarized states. In line with

recent studies, hippocampal activity displayed a similar alternation pattern. Importantly, we found a tendency for thalamic up-states to initiate and end ahead of hippocampal activity frames in close agreement with similar cortico-hippocampal measures. We also showed that the seemingly bidirectional communication between areas is present during periods of coincident depolarization. Given the well known reciprocal connectivity between cortex and thalamus, our data suggest that thalamic activity might play a role in the coordination of cortico-hippocampal replay events. Indeed, a recent study in anesthetized rats suggests that the firing mode displayed by thalamic cells has the ability to modify the depolarization state in cortical circuits (Hirata & Castro-Alamancos 2010). In addition, it has been demonstrated that spindle oscillations are produced in the thalamus and projected to cortex (Steriade et al. 1993). The fact that we find correlations between thalamic and hippocampal activity opens the possibility that the thalamus could bias the selection of cells that participate in both cortical and hippocampal replay.

In chapter 3, we investigated the temporal structure of thalamic HD cell activity during REM. While it has been long recognized that individual thalamic neurons display a tonic firing mode during REM (Paré et al. 1990; Steriade 1992), little is known about their ensemble activity. We were able to demonstrate that sets of HD cells encode continuous heading trajectories resembling awake profiles. In addition, we showed that individual neurons within the ensemble fire in a manner consistent with the decoded orientation. In other words, the trajectories were not simply the reflection of one cell dominating the activity of others but rather, the result of cohesive activity among thalamic cells. Importantly, cells during REM displayed the same degree of ensemble correspondence as during

maze running. Suggesting that the decoded REM orientation trajectories were related to awake behavior, we showed that the correlation between angular velocity and theta power introduced by the animals' behavior during track running was replicated during REM. We also showed that HD and place cells concurrently represented similar ambulatory states during REM. Because the specific spatial content differed between thalamus and hippocampus, our results suggest the possibility that REM activity might reflect the evaluation of alternative routes or the reactivation of earlier behaviors with similar navigational structures. Our results strongly suggest the active participation of thalamic activity in internal processes during sleep.

Some of the findings of the present work open several intriguing questions that warrant additional exploration. For instance, despite lack of thalamic replay we cannot rule out passive contributions of thalamic activity to hippocampal awake replay. Experiments in which thalamic activity is directly manipulated during awake behavior could provide a way to unmask its potential participation in hippocampal replay.

Our results in conjunction with recent findings showing that replay also represent paths never experienced by rats allow for the speculation that awake replay might be the result of interactions with brain areas directly involved with the active evaluation or planning of routes. Experiments in which cortical areas such as the retrosplenial cortex, posterior parietal cortex or prefrontal cortex are also monitored during navigation could provide useful information to better understand awake replay.

Other interesting questions arising from this work are: to what extent do task contingencies condition the re-expression of hippocampal firing patterns during REM? Do enhanced associations between hippocampus and prefrontal cortex result in stronger REM replay patterns? Are tasks with similar navigational structures compared during REM periods? The answer to these questions would benefit from multi-site recordings in which tasks that actively engage prefrontal-hippocampal interactions are employed. In general, the simultaneous combination of multiple experimental techniques will be necessary tools in answering the remaining questions.

## References

- Addis, D. R.; Wong, A. T. & Schacter, D. L.(2007). *Remembering the past and imagining the future: common and distinct neural substrates during event construction and elaboration.*, *Neuropsychologia* 45 :1363-1377.
- Aggleton, J. P.(2008). *EPS Mid-Career Award 2006. Understanding anterograde amnesia: disconnections and hidden lesions.*, *Q J Exp Psychol (Colchester)* 61 :1441-1471.
- Aggleton, J. P.; Neave, N.; Nagle, S. & Hunt, P. R.(1995). *A comparison of the effects of anterior thalamic, mamillary body and fornix lesions on reinforced spatial alternation.*, *Behav Brain Res* 68 :91-101.
- Anderson, M. P.; Mochizuki, T.; Xie, J.; Fischler, W.; Manger, J. P.; Talley, E. M.; Scammell, T. E. & Tonegawa, S.(2005). *Thalamic Cav3.1 T-type Ca<sup>2+</sup> channel plays a crucial role in stabilizing sleep.*, *Proc Natl Acad Sci U S A* 102 :1743-1748.
- Bal, T.; von Krosigk, M. & McCormick, D. A.(1995). *Synaptic and membrane mechanisms underlying synchronized oscillations in the ferret lateral geniculate nucleus in vitro.*, *J Physiol* 483 ( Pt 3) :641-663.
- Battaglia, F. P.; Sutherland, G. R. & McNaughton, B. L.(2004). *Local sensory cues and place cell directionality: additional evidence of prospective coding in the hippocampus.*, *J Neurosci* 24 :4541-4550.
- Brown, J. E.; Yates, B. J. & Taube, J. S.(2002). *Does the vestibular system contribute to head direction cell activity in the rat?*, *Physiol Behav* 77 : 743-748.
- Buckner, R. L.(2010). *The role of the hippocampus in prediction and imagination.*, *Annu Rev Psychol* 61 :27-48, C1-8.
- Buhl, D. L.; Harris, K. D.; Hormuzdi, S. G.; Monyer, H. & Buzsáki, G.(2003). *Selective impairment of hippocampal gamma oscillations in connexin-36 knock-out mouse in vivo.*, *J Neurosci* 23 :1013-1018.
- Burikov, A. A. & Yul, B.(1999). *The activity of thalamus and cerebral cortex neurons in rabbits during "slow wave-spindle" EEG complexes.*, *Neurosci Behav Physiol* 29 :143-149.
- Buzsáki, G.(1989). *Two-stage model of memory trace formation: a role for "noisy" brain states.*, *Neuroscience* 31 :551-570.

Buzsáki, G.; Leung, L. W. & Vanderwolf, C. H.(1983). *Cellular bases of hippocampal EEG in the behaving rat.*, Brain Res 287 :139-171.

Byrne, P.; Becker, S. & Burgess, N.(2007). *Remembering the past and imagining the future: a neural model of spatial memory and imagery.*, Psychol Rev 114 :340-375.

Calton, J. L.; Stackman, R. W.; Goodridge, J. P.; Archey, W. B.; Dudchenko, P. A. & Taube, J. S.(2003). *Hippocampal place cell instability after lesions of the head direction cell network.*, J Neurosci 23 :9719-9731.

Calton, J. L. & Taube, J. S.(2009). *Where am I and how will I get there from here? A role for posterior parietal cortex in the integration of spatial information and route planning.*, Neurobiol Learn Mem 91 :186-196.

Cho, J. & Sharp, P. E.(2001). *Head direction, place, and movement correlates for cells in the rat retrosplenial cortex.*, Behav Neurosci 115 :3-25.

Csicsvari, J.; Hirase, H.; Czurko, A. & Buzsáki, G.(1998). *Reliability and state dependence of pyramidal cell-interneuron synapses in the hippocampus: an ensemble approach in the behaving rat.*, Neuron 21 : 179-189.

Csicsvari, J.; Hirase, H.; Czurkó, A.; Mamiya, A. & Buzsáki, G.(1999). *Fast network oscillations in the hippocampal CA1 region of the behaving rat.*, J Neurosci 19 :RC20.

Csicsvari, J.; O'Neill, J.; Allen, K. & Senior, T.(2007). *Place-selective firing contributes to the reverse-order reactivation of CA1 pyramidal cells during sharp waves in open-field exploration.*, Eur J Neurosci 26 :704-716.

Davidson, T. J.; Kloosterman, F. & Wilson, M. A.(2009). *Hippocampal replay of extended experience.*, Neuron 63 :497-507.

Destexhe, A.; McCormick, D. A. & Sejnowski, T. J.(1993). *A model for 8-10 Hz spindling in interconnected thalamic relay and reticularis neurons.*, Biophys J 65 :2473-2477.

Diba, K. & Buzsáki, G.(2007). *Forward and reverse hippocampal place-cell sequences during ripples.*, Nat Neurosci 10 :1241-1242.

Ego-Stengel, V. & Wilson, M. A.(2009). *Disruption of ripple-associated hippocampal activity during rest impairs spatial learning in the rat.*, Hippocampus 20:1-10.

Ekstrom, A. D.; Caplan, J. B.; Ho, E.; Shattuck, K.; Fried, I. & Kahana, M. J. (2005). *Human hippocampal theta activity during virtual navigation.*, Hippocampus 15 :881-889.

Fisher, N. I., 1993. *Statistical Analysis of Circular Data*. Cambridge University Press, .

Foster, D. J. & Wilson, M. A.(2006). *Reverse replay of behavioural sequences in hippocampal place cells during the awake state.*, Nature 440 :680-683.

Fyhn, M.; Hafting, T.; Witter, M. P.; Moser, E. I. & Moser, M.-B.(2008). *Grid cells in mice.*, Hippocampus 18 :1230-1238.

Fyhn, M.; Molden, S.; Witter, M. P.; Moser, E. I. & Moser, M.-B.(2004). *Spatial representation in the entorhinal cortex.*, Science 305 :1258-1264.

Girardeau, G.; Benchenane, K.; Wiener, S. I.; Buzsáki, G. & Zugaro, M. B. (2009). *Selective suppression of hippocampal ripples impairs spatial memory.*, Nat Neurosci 12 :1222-1223.

Golob, E. J. & Taube, J. S.(1997). *Head direction cells and episodic spatial information in rats without a hippocampus.*, Proc Natl Acad Sci U S A 94 : 7645-7650.

Goodridge, J. P. & Taube, J. S.(1997). *Interaction between the postsubiculum and anterior thalamus in the generation of head direction cell activity.*, J Neurosci 17 :9315-9330.

Gupta, A. S.; van der Meer, M. A. A.; Touretzky, D. S. & Redish, A. D. (2010). *Hippocampal replay is not a simple function of experience.*, Neuron 65 :695-705.

Hahn, T. T. G.; Sakmann, B. & Mehta, M. R.(2006). *Phase-locking of hippocampal interneurons' membrane potential to neocortical up-down states.*, Nat Neurosci 9 :1359-1361.

Hahn, T. T. G.; Sakmann, B. & Mehta, M. R.(2007). *Differential responses of hippocampal subfields to cortical up-down states.*, Proc Natl Acad Sci U S A 104 :5169-5174.

Hassabis, D.; Kumaran, D. & Maguire, E. A.(2007). *Using imagination to understand the neural basis of episodic memory.*, J Neurosci 27 :14365-14374.

- Hassabis, D.; Kumaran, D.; Vann, S. D. & Maguire, E. A.(2007). *Patients with hippocampal amnesia cannot imagine new experiences.*, Proc Natl Acad Sci U S A 104 :1726-1731.
- Hasselmo, M. E.(2009). *A model of episodic memory: mental time travel along encoded trajectories using grid cells.*, Neurobiol Learn Mem 92 : 559-573.
- Hirata, A. & Castro-Alamancos, M. A.(2010). *Neocortex network activation and deactivation states controlled by the thalamus.*, J Neurophysiol 103 :1147-1157.
- Hobson, J. A. & Pace-Schott, E. F.(2002). *The cognitive neuroscience of sleep: neuronal systems, consciousness and learning.*, Nat Rev Neurosci 3 :679-693.
- Hoffmann, M. B.; Stadler, J.; Kanowski, M. & Speck, O.(2009). *Retinotopic mapping of the human visual cortex at a magnetic field strength of 7T.*, Clin Neurophysiol 120 :108-116.
- Ji, D. & Wilson, M. A.(2007). *Coordinated memory replay in the visual cortex and hippocampus during sleep.*, Nat Neurosci 10 :100-107.
- Johnson, A.; Seeland, K. & Redish, A. D.(2005). *Reconstruction of the postsubiculum head direction signal from neural ensembles.*, Hippocampus 15 :86-96.
- Jones, M. W. & Wilson, M. A.(2005). *Theta rhythms coordinate hippocampal-prefrontal interactions in a spatial memory task.*, PLoS Biol 3 :e402.
- Josseaux, T.; Calvier, E. A.; Duport, B. D.; Lebouvier, T.; Mathieu, G. P.; de Kersaint Gilly, A. & Desal, H.(2007). *[Acute anterograde amnesia by infarction of the mamillothalamic tracts]*, J Neuroradiol 34 :59-62.
- Karlsson, M. P. & Frank, L. M.(2009). *Awake replay of remote experiences in the hippocampus.*, Nat Neurosci 12 :913-918.
- Klausberger, T.; Magill, P. J.; Márton, L. F.; Roberts, J. D. B.; Cobden, P. M.; Buzsáki, G. & Somogyi, P.(2003). *Brain-state- and cell-type-specific firing of hippocampal interneurons in vivo.*, Nature 421 :844-848.
- Klausberger, T. & Somogyi, P.(2008). *Neuronal diversity and temporal dynamics: the unity of hippocampal circuit operations.*, Science 321 :53-57.

Knierim, J. J.; Kudrimoti, H. S. & McNaughton, B. L.(1998). *Interactions between idiothetic cues and external landmarks in the control of place cells and head direction cells.*, J Neurophysiol 80 :425-446.

Kopelman, M. D.; Thomson, A. D.; Guerrini, I. & Marshall, E. J.(2009). *The Korsakoff syndrome: clinical aspects, psychology and treatment.*, Alcohol Alcohol 44 :148-154.

Kreiman, G.; Koch, C. & Fried, I.(2000). *Imagery neurons in the human brain.*, Nature 408 :357-361.

Lee, A. K. & Wilson, M. A.(2002). *Memory of sequential experience in the hippocampus during slow wave sleep.*, Neuron 36 :1183-1194.

Leutgeb, J. K.; Leutgeb, S.; Treves, A.; Meyer, R.; Barnes, C. A.; McNaughton, B. L.; Moser, M.-B. & Moser, E. I.(2005a). *Progressive transformation of hippocampal neuronal representations in "morphed" environments.*, Neuron 48 :345-358.

Leutgeb, S.; Leutgeb, J. K.; Barnes, C. A.; Moser, E. I.; McNaughton, B. L. & Moser, M.-B.(2005b). *Independent codes for spatial and episodic memory in hippocampal neuronal ensembles.*, Science 309 :619-623.

Louie, K. & Wilson, M. A.(2001). *Temporally structured replay of awake hippocampal ensemble activity during rapid eye movement sleep.*, Neuron 29 :145-156.

Maier, N.; Güldenagel, M.; Söhl, G.; Siegmund, H.; Willecke, K. & Draguhn, A.(2002). *Reduction of high-frequency network oscillations (ripples) and pathological network discharges in hippocampal slices from connexin 36-deficient mice.*, J Physiol 541 :521-528.

Maier, N.; Nimmrich, V. & Draguhn, A.(2003). *Cellular and network mechanisms underlying spontaneous sharp wave-ripple complexes in mouse hippocampal slices.*, J Physiol 550 :873-887.

Marks, G. A. & Roffwarg, H. P.(1993). *Spontaneous activity in the thalamic reticular nucleus during the sleep/wake cycle of the freely-moving rat.*, Brain Res 623 :241-248.

Markus, E. J.; Qin, Y. L.; Leonard, B.; Skaggs, W. E.; McNaughton, B. L. & Barnes, C. A.(1995). *Interactions between location and task affect the spatial and directional firing of hippocampal neurons.*, J Neurosci 15 : 7079-7094.

McCarley, R. W.; Benoit, O. & Barrionuevo, G.(**1983**). *Lateral geniculate nucleus unitary discharge in sleep and waking: state- and rate-specific aspects.*, J Neurophysiol 50 :798-818.

McCormick, D. A. & Pape, H. C.(**1990**). *Properties of a hyperpolarization-activated cation current and its role in rhythmic oscillation in thalamic relay neurones.*, J Physiol 431 :291-318.

McNaughton, B. L.; Barnes, C. A. & O'Keefe, J.(**1983**). *The contributions of position, direction, and velocity to single unit activity in the hippocampus of freely-moving rats.*, Exp Brain Res 52 :41-49.

McNaughton, B. L.; Battaglia, F. P.; Jensen, O.; Moser, E. I. & Moser, M.-B. (**2006**). *Path integration and the neural basis of the 'cognitive map'.*, Nat Rev Neurosci 7 :663-678.

Mehta, M. R.(**2007**). *Cortico-hippocampal interaction during up-down states and memory consolidation.*, Nat Neurosci 10 :13-15.

Metcalf, M.; Xu, D.; Okuda, D. T.; Carvajal, L.; Srinivasan, R.; Kelley, D. A. C.; Mukherjee, P.; Nelson, S. J.; Vigneron, D. B. & Pelletier, D.(**2009**). *High-Resolution Phased-Array MRI of the Human Brain at 7 Tesla: Initial Experience in Multiple Sclerosis Patients.*, J Neuroimaging .

O'Keefe, J. & Dostrovsky, J.(**1971**). *The hippocampus as a spatial map. Preliminary evidence from unit activity in the freely-moving rat.*, Brain Res 34 :171-175.

O'Neill, J.; Senior, T. J.; Allen, K.; Huxter, J. R. & Csicsvari, J.(**2008**). *Reactivation of experience-dependent cell assembly patterns in the hippocampus.*, Nat Neurosci 11 :209-215.

Pace-Schott, E. F. & Hobson, J. A.(**2002**). *The neurobiology of sleep: genetics, cellular physiology and subcortical networks.*, Nat Rev Neurosci 3 :591-605.

Papez, J. W.(**1937**). *A proposed mechanism of emotion*, Arch Neurol Psychiatr 38 :725-734.

Paré, D.; Dossi, R. C. & Steriade, M.(**1991**). *Three types of inhibitory postsynaptic potentials generated by interneurons in the anterior thalamic complex of cat.*, J Neurophysiol 66 :1190-1204.

Paré, D.; Steriade, M.; Deschênes, M. & Bouhassira, D.(**1990**). *Prolonged enhancement of anterior thalamic synaptic responsiveness by*

*stimulation of a brain-stem cholinergic group.*, J Neurosci 10 :20-33.

Ramcharan, E. J.; Gnadt, J. W. & Sherman, S. M.(**2000**). *Burst and tonic firing in thalamic cells of unanesthetized, behaving monkeys.*, Vis Neurosci 17 :55-62.

Ramcharan, E. J.; Gnadt, J. W. & Sherman, S. M.(**2005**). *Higher-order thalamic relays burst more than first-order relays.*, Proc Natl Acad Sci U S A 102 :12236-12241.

Robert, C.; Guilpin, C. & Limoge, A.(**1999**). *Automated sleep staging systems in rats.*, J Neurosci Methods 88 :111-122.

Rose, G.; Diamond, D. & Lynch, G. S.(**1983**). *Dentate granule cells in the rat hippocampal formation have the behavioral characteristics of theta neurons.*, Brain Res 266 :29-37.

Sanchez-Panchuelo, R. M.; Francis, S.; Bowtell, R. & Schluppeck, D. (**2010**). *Mapping human somatosensory cortex in individual subjects with 7T functional MRI.*, J Neurophysiol .

Scoville, W. B. & Milner, B.(**2000**). *Loss of recent memory after bilateral hippocampal lesions. 1957.*, J Neuropsychiatry Clin Neurosci 12 :103-113.

Sharp, P. E.(**1996**). *Multiple spatial/behavioral correlates for cells in the rat postsubiculum: multiple regression analysis and comparison to other hippocampal areas.*, Cereb Cortex 6 :238-259.

Sharp, P. E. & Green, C.(**1994**). *Spatial correlates of firing patterns of single cells in the subiculum of the freely moving rat.*, J Neurosci 14 : 2339-2356.

Siapas, A. G.; Lubenov, E. V. & Wilson, M. A.(**2005**). *Prefrontal phase locking to hippocampal theta oscillations.*, Neuron 46 :141-151.

Siapas, A. G. & Wilson, M. A.(**1998**). *Coordinated interactions between hippocampal ripples and cortical spindles during slow-wave sleep.*, Neuron 21 :1123-1128.

Solstad, T.; Moser, E. I. & Einevoll, G. T.(**2006**). *From grid cells to place cells: a mathematical model.*, Hippocampus 16 :1026-1031.

Stackman, R. W.; Clark, A. S. & Taube, J. S.(**2002**). *Hippocampal spatial representations require vestibular input.*, Hippocampus 12 :291-303.

Stackman, R. W.; Golob, E. J.; Bassett, J. P. & Taube, J. S.(**2003**). *Passive transport disrupts directional path integration by rat head direction cells.*, J Neurophysiol 90 :2862-2874.

Stackman, R. W. & Taube, J. S.(**1997**). *Firing properties of head direction cells in the rat anterior thalamic nucleus: dependence on vestibular input.*, J Neurosci 17 :4349-4358.

Stackman, R. W. & Taube, J. S.(**1998**). *Firing properties of rat lateral mammillary single units: head direction, head pitch, and angular head velocity.*, J Neurosci 18 :9020-9037.

Steriade, M.(**1992**). *Basic mechanisms of sleep generation.*, Neurology 42 :9-17; discussion 18.

Steriade, M.(**2004**). *Acetylcholine systems and rhythmic activities during the waking--sleep cycle.*, Prog Brain Res 145 :179-196.

Steriade, M.; Contreras, D.; Dossi, R. C. & Nuñez, A.(**1993**). *The slow (< 1 Hz) oscillation in reticular thalamic and thalamocortical neurons: scenario of sleep rhythm generation in interacting thalamic and neocortical networks.*, J Neurosci 13 :3284-3299.

Steriade, M.; Deschênes, M.; Domich, L. & Mulle, C.(**1985**). *Abolition of spindle oscillations in thalamic neurons disconnected from nucleus reticularis thalami.*, J Neurophysiol 54 :1473-1497.

Steriade, M.; Nuñez, A. & Amzica, F.(**1993**). *Intracellular analysis of relations between the slow (< 1 Hz) neocortical oscillation and other sleep rhythms of the electroencephalogram.*, J Neurosci 13 :3266-3283.

Taube, J. S.(**1995**). *Head direction cells recorded in the anterior thalamic nuclei of freely moving rats.*, J Neurosci 15 :70-86.

Taube, J. S. & Burton, H. L.(**1995**). *Head direction cell activity monitored in a novel environment and during a cue conflict situation.*, J Neurophysiol 74 :1953-1971.

Taube, J. S.; Kesslak, J. P. & Cotman, C. W.(**1992**). *Lesions of the rat postsubiculum impair performance on spatial tasks.*, Behav Neural Biol 57 :131-143.

Taube, J. S.; Muller, R. U. & Ranck, J. B.(**1990**). *Head-direction cells recorded from the postsubiculum in freely moving rats. II. Effects of environmental manipulations.*, J Neurosci 10 :436-447.

- Thomas, B. P.; Welch, E. B.; Niederhauser, B. D.; Whetsell, W. O.; Anderson, A. W.; Gore, J. C.; Avison, M. J. & Creasy, J. L.(2008). *High-resolution 7T MRI of the human hippocampus in vivo.*, J Magn Reson Imaging 28 :1266-1272.
- Toft, P.(1996). *The Radon Transform - Theory and Implementation*, Technical University of Denmark.
- Vann, S. D. & Aggleton, J. P.(2004). *The mammillary bodies: two memory systems in one?*, Nat Rev Neurosci 5 :35-44.
- Vann, S. D.; Aggleton, J. P. & Maguire, E. A.(2009). *What does the retrosplenial cortex do?*, Nat Rev Neurosci 10 :792-802.
- Vann, S. D.; Saunders, R. C. & Aggleton, J. P.(2007). *Distinct, parallel pathways link the medial mammillary bodies to the anterior thalamus in macaque monkeys.*, Eur J Neurosci 26 :1575-1586.
- Vertes, R. P.; Albo, Z. & Prisco, G. V. D.(2001). *Theta-rhythmically firing neurons in the anterior thalamus: implications for mnemonic functions of Papez's circuit.*, Neuroscience 104 :619-625.
- Vertes, R. P.; Hoover, W. B. & Prisco, G. V. D.(2004). *Theta rhythm of the hippocampus: subcortical control and functional significance.*, Behav Cogn Neurosci Rev 3 :173-200.
- Warburton, E. C. & Aggleton, J. P.(1999). *Differential deficits in the Morris water maze following cytotoxic lesions of the anterior thalamus and fornix transection.*, Behav Brain Res 98 :27-38.
- Warburton, E. C.; Baird, A. L.; Morgan, A.; Muir, J. L. & Aggleton, J. P. (2000). *Disconnecting hippocampal projections to the anterior thalamus produces deficits on tests of spatial memory in rats.*, Eur J Neurosci 12 : 1714-1726.
- der Werf, Y. D. V.; Jolles, J.; Witter, M. P. & Uylings, H. B. M.(2003). *Contributions of thalamic nuclei to declarative memory functioning.*, Cortex 39 :1047-1062.
- Whitlock, J. R.; Sutherland, R. J.; Witter, M. P.; Moser, M.-B. & Moser, E. I. (2008). *Navigating from hippocampus to parietal cortex.*, Proc Natl Acad Sci U S A 105 :14755-14762.
- Wierzynski, C. M.; Lubenov, E. V.; Gu, M. & Siapas, A. G.(2009). *State-dependent spike-timing relationships between hippocampal and*

*prefrontal circuits during sleep.*, Neuron 61 :587-596.

Wilson, M. A. & McNaughton, B. L.(**1994**). *Reactivation of hippocampal ensemble memories during sleep.*, Science 265 :676-679.

Wolansky, T.; Clement, E. A.; Peters, S. R.; Palczak, M. A. & Dickson, C. T. (**2006**). *Hippocampal slow oscillation: a novel EEG state and its coordination with ongoing neocortical activity.*, J Neurosci 26 :6213-6229.

Yoder, R. M. & Taube, J. S.(**2009**). *Head direction cell activity in mice: robust directional signal depends on intact otolith organs.*, J Neurosci 29 :1061-1076.

Zhang, K.; Ginzburg, I.; McNaughton, B. L. & Sejnowski, T. J.(**1998**). *Interpreting neuronal population activity by reconstruction: unified framework with application to hippocampal place cells.*, J Neurophysiol 79 :1017-1044.

Andersen, P. (Ed.),**2007**. *The hippocampus book*. Oxford University Press, .

Jones, E. G. (Ed.),**2007**. *The Thalamus*. Cambridge University Press, .